Differential internalization of hu14.18-IL2 immunocytokine by NK and tumor cell: impact on conjugation, cytotoxicity and targeting

Ilia N. Buhtoiarov[1,2*], Zane C. Neal[1*†], Jacek Gan[*], Tatiana N. Buhtoiarova[*], Manish S. Patankar[§], Jennifer A.A. Gubbels[§], Jacquelyn A. Hank[*], Brett Yamane[*], Alexander L. Rakhmilevich[*], Ralph A. Reisfeld[¶], Stephen D. Gillies[‖], and Paul M. Sondel[*#].

[*]Department of Human Oncology and The University of Wisconsin Paul P. Carbone Comprehensive Cancer Center, University of Wisconsin, Madison, WI; [†]Mirus Bio Corporation, Madison WI, [§]Department of Obstetrics and Gynecology, UW-Madison; [¶]The Scripps Research Institute, La Jolla CA, [‖]Provenance Biopharmaceuticals, Waltham MA; and [#]Department of Pediatrics, UW-Madison.

Summary sentence: Internalization of hu14.18-IL2 occurs through IL2 receptors on NK effectors and GD_2 antigen on tumor targets, with slower kinetics on tumor accounting for effective NK/tumor interactions.

Running title: Internalization of hu14.18-IL2 by NK and tumor cells.

Corresponding author: Professor Paul M. Sondel, UW Carbone Cancer Center, 4159 MACC Fund UW Childhood Cancer Research Wing, WIMR, 1111 Highland Avenue, Madison WI, 53705-2275, phone: (608) 263-9069, fax: (608) 263-4226, e-mail: pmsondel@facstaff.wisc.edu

Key words: immune synapse, GD_2, IL2R, NK cells, melanoma, neuroblastoma

Counts:

Total – 61056 characters

Figures – 9 total; 1 color figure

References – 43

Abstract – 202 words

Summary sentence – 26 words

Abbreviations Page

Abbreviations used in this paper: IC, immunocytokine; hu14.18-IL2 IC, humanized 14.18-IL2 immunocytokine; GD_2, GD_2 disialoganglioside; NB, neuroblastomas; HS, human serum; IL2R, interleukin-2 receptor; IT, intratumorally; CFSE, carboxyfluoroscein succinimidyl ester; BODIPY, SE 6-(((4,4-difluoro-5-(2-thienyl)-4-bora-3a,4a-diaza-*s*-indacene-3-yl) styryloxy)acetyl) aminohexanoic acid, succinimidyl ester.

Abstract

The hu14.18-IL2 (EMD 273063) immunocytokine (IC), consisting of a GD_2-specific mAb genetically engineered to two molecules of IL2, is in clinical trials for treatment of GD_2-expressing tumors. Anti-tumor activity of IC *in vivo* and *in vitro* involves natural killer (NK) cells. We studied the kinetics of retention of IC on the surface of human $CD25^+CD16^-$NK cell lines (NKL and RL12) and GD_2^+M21 melanoma after IC binding to the cells via IL2R and GD_2, respectively. For NK cells, ~50% of IC was internalized by 3 h, and ~90% by 24 h of cell culture. The decrease of surface IC levels on NK cells correlated with the loss of their ability to bind to tumor cells and mediate ADCC *in vitro*. Unlike NK cells, M21 cells retained ~70% of IC on the surface following 24 h of culture and maintained the ability to become conjugated and lysed by NK cells. When NKL cells were injected into M21-bearing SCID mice, intratumoral delivery of IC augmented NK cell migration into the tumor. These studies demonstrate that once IC binds to tumor, it is present on the tumor surface for a prolonged time, inducing the recruitment of NK cells to the tumor site followed by tumor cell killing.

Introduction.

The humanized 14.18-IL2 immunocytokine (hu14.18-IL2 IC) is the second-generation form of the original ch14.18-IL2 [1]. It is comprised of the humanized 14.18 anti-disialoganglioside (GD_2) antibody V regions that are joined at the genetic level to the human C kappa and C gamma heavy chains, the latter of which is fused at the carboxyl terminus to human IL2. The hu14.18 mAb can recognize GD_2 expressed on human melanomas [2, 3] and neuroblastomas (NB) [4, 5], and potentially on some other human tumors expressing GD_2, including small cell lung cancers [6], certain sarcomas [7, 8] and intracranial tumors [9]. Presently, IC is being tested in clinical trials in NB and melanoma [10, 11]. In these clinical studies it was found that NK cells from patients mediate more potent lysis of $GD2^+$ tumor cells *in vitro* when obtained after they received *in vivo* treatment with hu14.18-IL2 [10]. In A/J mice bearing NXS2, a GD_2^+ mouse NB, treatment with the hu14.18-IL2 IC induced strong NK cell-dependent antitumor responses against local and metastatic disease which significantly exceeded the antitumor effects of the mAb combined with IL2 [12, 13].

Following administration of radiolabeled ICs *in vivo*, localization to the tumor has been documented [14, 15]. This phenomenon is appreciably more pronounced when IC is injected intratumorally (IT) [16]. Accumulation of IC in the tumor is accompanied by augmented migration of the immune cells into the tumor [17]. However, it remains unclear whether IC accumulates in the tumor passively, while being bound to IL2- or Fc-receptor expressing T cells and NK cells migrating to the tumor, or whether accumulation of IC in the tumor occurs first via direct binding to tumor antigen, followed by active recruitment and adhesion of T and NK cells to the tumor via binding of their IL2R to the IL2-component of IC.

Once bound to the cell surface, the IC would be subject to biological processes of the cell

membrane, including possible internalization via antigen or IL2R internalization. Indeed, IL2Rs become rapidly internalized upon binding IL2 molecules [18-20]. Both high-affinity (i.e. composed of α [CD25]-, β [CD122]- and γ [CD132]-subunits) and intermediate-affinity (i.e. composed of only β- and γ-subunits) IL2Rs can be internalized upon IL2 binding [21, 22]. Human peripheral blood-derived NK cells express intermediate-affinity IL2Rs but also can express high-affinity IL2Rs upon activation [23-25]. Similarly to IL2Rs, ganglioside antigens on certain types of tumor cells can also mediate internalization of monoclonal antibody-surface antigen complexes [26, 27].

In this study we evaluated the stability of hu14.18-IL2 IC on the surface of human $GD2^+$ tumor cells (M21 melanoma) and $IL2R^+$NK cells (NKL and RL12 human NK cell lines). We found that melanoma and NK cells internalize hu14.18-IL2 IC, but NK cells internalized IC at a much higher rate. It was also found that internalization of cell-surface bound IC by NK cells diminished their subsequent ability to conjugate to $GD2^+$ M21 cells and effectively lyse them. IC internalization by M21 cells (as well as by mouse NXS2 NB cells) occurred at a significantly slower rate; tumor cells pre-armed with IC could be effectively targeted and lysed by NK cells at any of the time-points tested. When hu14.18-IL2 IC was injected intratumorally, it was detectable on the M21 tumor cell surface even 24 hr after IC injection, and coincided with augmented migration of resident and adoptively-transferred NK cells into the tumor. Thus, the stability of hu14.18-IL2 IC binding to both tumor cells and immune effectors, and the relative residence time on the cell surface, is affected by differences in internalization between the antibody target and the cytokine receptor.

Materials and Methods

Hu14.18 Ab and IC. The GD_2-specific humanized 14.18 Ab and 14.18-IL2 IC, that have been described previously [1, 28, 29], were obtained from EMD-Lexigen Research Center (Billerica, MA). One microgram of hu14.18-IL2 IC contains approximately 3000 IU of IL-2 activity, as previously determined [30]. Custom labeling of hu14.18 Ab or hu14.18-IL2 IC with FITC was preformed by using EZ-Label FITC protein labeling kit (53004) (PIERCE, Rockford, IL). The products were purified by using Slide-A-Lyzer Mini Dialysis Unit (3,500 MWCO) (also from PIERCE).

Cell lines. NKL [31] and RL12 (a human serum-dependent subline of human leukemia NKL, obtained from Dr. Paul Leibson of the Mayo Clinic, Rochester MN) human NK cell lines were grown in complete RPMI-1640 cell culture medium supplemented with 10% FBS (Sigma-Aldrich, St. Louis, MO), 5% of fresh human serum (HS) obtained from healthy donors, 2 mM L-glutamine, 100 U/ml penicillin/streptomycin, and 25-250 U/ml of exogenous recombinant human IL2 (TECIN; Hoffmann-La Roche, Inc., Nutley, NJ) at 37°C in a humidified 5% CO_2 atmosphere. Under certain experimental conditions, NKL and RL12 cells were grown in complete medium but without exogenous IL2 for 24 hr prior to using in experiments. K562 human chronic myelogenous leukemia, M21 human melanoma, L5178Y mouse T cell lymphoma, CT26 mouse colon carcinoma cell lines were cultured in complete RPMI-1640 cell culture medium formulated as detailed above but without human serum and IL2. NXS2 mouse NB cell line was grown in complete DMEM medium.

Labeling of cells with intravital dyes. CFSE [carboxyfluoroscein succinimidyl ester, excitation: 490 nm, emission: 518 nm] and BODIPY 630/650-X, [SE 6-(((4,4-difluoro-5-(2-thienyl)-4-bora-3a,4a-diaza-*s*-indacene-3-yl)styryloxy)acetyl) aminohexanoic acid, succinimidyl ester,

excitation: 630 nm, emission: 650 nm] were purchased from Invitrogen (Carlsbad, CA). Prior to labeling, the cells were washed twice with room temperature-warm PBS to eliminate serum residua, re-suspended in 10 ml of 37^{o}C-warm PBS supplemented with 5 mM of CFSE or 1 mM of BODIPY, and incubated for 15 min at 37^{0}C. The labeled cells were washed once with ice-cold 10% FCS PBS (to neutralize free, cell-unbound label), resuspended in complete cell culture medium and thereafter incubated at 37°C in a humidified 5% CO_2 atmosphere for 0-3 days prior to using in *in vitro* and *in vivo* experiments.

Arming cells with hu14.18-IL2 IC. M21, NXS2, NKL, RL12 and L5178Y cells (3x10^{6}/0.1 ml) were incubated for 1 hr on ice with 2 μg/sample of FITC-labeled hu14.18-IL2 IC followed by cell washing with ice-cold PBS + 2%FCS.

Flow cytometry. The following anti-human or anti-mouse antibodies were used: anti-mouse CD16/CD32-FITC (clone 2.4G2); anti-mouse CD25-FITC (3C7); anti-human CD16-FITC (3G8), anti-human CD25-FITC (M-A251), all from BDBioscience; anti-mouse CD49b-FITC (DX5) was purchased from eBioscience (San Diego, CA). PE- or Allophycocyanin (APC)-conjugated polyclonal goat anti-human IgG (G-α-H) were purchased from eBioscience or Open Biosystems (Huntsville, AL). The cells (3x10^{5}/0.05 ml) or single cell tumor preparations were incubated on ice for 40 min with 1 μg/ml of hu14.18 Ab, hu14.18-IL2 IC, other specific antibody or isotype-matched control IgGs, and the unbound antibody was washed off. The flow cytometry analysis was performed on CellQuest software of FacsCalibur flow cytometer (BD Biosciences). Analysis of acquired data was performed using FlowJo software (Tree Star, Inc).

Mean Fluorescence Intensity (MFI) ratio calculation. The MFI ratio was calculated by dividing the flow cytometric MFI value of cells stained with antigen-specific mAb by the MFI value for the same cells stained with isotype-matched control immunoglobulin. This approach

allows for comparison of multiple test samples within a group and between different groups.

Effector cell – target cell conjugate formation essay. CFSE-labeled NKL or RL12 cells ($1.5x10^5$/0.1) and BODIPY 630/650-labeled M21 melanoma cells ($1.5x10^5$/0.1 ml, unless indicated otherwise) were mixed together in flow cytometry sample tubes (Falcon-35 5-ml polystyrene tubes) in complete RPMI-1640 medium with or without 1 μg/ml hu14.18 Ab, 3000 U/ml IL2 (the amount of IL2 contained in 1 μg of IC), 1 μg/ml hu14.18 Ab + 3000 U/ml IL2, 1 μg/ml hu14.18-IL2 IC or 1 μg/ml hu14.18-IL2 IC+ 3000 U/ml IL2, and loose pellet was formed by the cell mixture centrifugation at 500 rpm/1 min followed by incubation of the pelleted cells for 30 min at 37^0C. Under certain experimental conditions, the tumor cells or NK cells were pre-armed with hu14.18-IL2 IC, as described above, prior to mixing together in the flow cytometry tubes for conjugate formation. After 30 min of incubation the pellet was gently agitated by tapping the tube on the firm surface and the cells were tested by flow cytometry for M21-NK cell conjugate formation.

IC internalization assay. M21, NXS2, NKL, RL12, L5178Y cells ($3x10^6$/0.1 ml of complete cell culture medium without HS and IL2) were armed with 2 μg of FITC-conjugated IC on ice for 1 hr, and the excess of IC was removed by cell washing in ice-cold PBS. The cells were re-suspended in complete medium without HS and IL2, distributed into 1 ml polypropylene eppendorf tubes and placed on 37^0C water in a humidified 5% CO_2 atmosphere. After 0-24 hr of IC-armed cell incubation, the pellets were harvested by pipetting, washed with ice-cold PBS to remove the shed IC and thereafter labeled with secondary APC-conjugated goat anti-human IgG for any IC still present on the surface. The double-labeled cells were analyzed for both FITC and APC by flow cytometry. As a control for IC-FITC, a mouse anti-human IgG-FITC was used. The MFI ratios were determined by dividing FITC/APC MFI values of samples that were armed

with IC-FITC and later stained with secondary goat anti-human IgG-APC by the FITC/APC MFI value of the sample that was armed with mouse anti-human IgG-FITC and goat anti-human IgG-APC. This approach allows for comparison of multiple samples within a group and between different groups-delete. The kinetics of IC internalization is expressed as % of relative retention of FITC/APC MFI values of samples incubated at 37^0C for 0.5-25 hr from the maximal values of FITC/APC MFI ratios of the sample that was incubated at 37^0C for 0 hr.

Cytotoxicity assay. The 4-hour ^{51}Cr-release cytotoxicity assay was performed as described previously [32]. $1.5x10^5$, $0.75x10x^5$ or $0.375x10^5$ NKL or RL12 effector NK cells were mixed in quadruplicates in U-bottom microwell cell culture clusters (Costar) with $5x10^3$ cells/well of ^{51}Cr-pulsed GD_2^+M21 or GD_2^-K562 target cells in 30:1, 15:1 or 7.5 effector-to-target (E:T) ratios, respectively, in complete RPMI1640 medium (without HS) with or without 1 µg/ml hu14.18 Ab, 3000 U/ml IL2, 1 µg/ml hu14.18 Ab + 3000 U/ml IL2, 1 µg/ml hu14.18-IL2 IC or 1 µg/ml hu14.18-IL2 IC+ 3000 U/ml IL2. Under certain experimental conditions, effector or target cells were pre-armed with hu14.18-IL2 IC, as described above, prior to using in the cytotoxicity assay. In other experiments, $1x10^5$/ml NK cells were pre-incubated on ice with 10 µg/ml anti-CD25 mAb (anti-TAC, mouse IgG1, clone GL439) for 1 hr followed by two washings with ice-cold PBS prior to being admixed with the tumor target cells. After the cells were mixed in wells, the loose pellets were formed by 0.5 min centrifugation at 100 rpm followed by incubation of the pelleted cells for 4 min at 37^0C in 5% CO_2 humidified atmosphere. After 4 hr incubation, the supernatant was harvested utilizing the Skatron harvesting system (Skatron, McLean, VA) and cytotoxicity values (%) were calculated at each E/T ratio as reported previously [33].

In vivo tumor model and intratumoral (IT) treatment. Eight to ten week old SCID mice (Harlan Sprague Dawley, Madison, WI), were housed, cared for, and used in accordance with the

Guide for Care and Use of Laboratory Animals (NIH publication 86-23, National Institutes of Health, Bethesda, MD, 1985).

M21 cells ($5x10^6$/0.1 ml) were implanted subcutaneously into abdominal flank, and tumor growth was monitored. On day 27, when average tumor size was 200-250 mm^3 (7-9 mm in diameter), the animals were randomly divided into 3 groups (n=3/group) and treated IT with 3 daily injections of 50 µl of PBS (PBS x 3, group 1), two days of 50 µl PBS and one with 10 µg hu14.18-IL2 IC/0.05 ml PBC (PBS x 2/IC x 1, group 2), or 3 consecutive daily injections of 10 µg IC/0.05 ml PBC (IC x 3, group 3). Immediately after the last injection of PBS (group 1) or IC (groups 2 and 3) all mice were injected intravenously (IV) with $5x10^6$/0.2 ml of BODIPY-labeled NKL cells. Twenty-four hours after NKL cell injection the animals were euthanized, the tumors were harvested and processed to a single cell suspension. The resultant cell samples from each mouse were tested by flow cytometry for prevalence of resident $CD49B^+$NK cells and implanted $BODIPY^+$NKL cells, as well as for presence of hu14.18-IL2 on the surface of tumor-infiltrating NK cells or tumor cells/non-tumor stroma cells.

Statistical analysis. A two-tailed Student's *t*-test was used to determine significance of differences between experimental and relevant control values within one experiment.

Results

Cell immunophenotype determines specificity of mechanism of hu14.18-IL2 IC binding.

The hu14.18-IL2 IC can bind to the cells expressing GD_2 antigen, via its antigen-binding site. It also can bind to cells expressing IL2Rs, via its Fc region-bound IL2 molecule, just as it can bind to cells expressing FcRs, via the Fc region of the mAb. To analyze potential interactions of IC with the effector and target cells used in this study, we first determined the GD_2, FcR and IL2R phenotype of two human NK cell lines, NKL and RL12, and well as two tumor cell lines, human M21 melanoma and mouse NXS2 NB (Fig. 1). Both of the NK cell lines constitutively express high levels of CD25 (IL2Rα chain) but very low levels of CD16 (FcRγIII) (Fig 1A, B), and neither expresses GD_2. In contrast, neither M21 nor NXS2 cells express CD25 or CD16 but both are recognized by the hu14.18 mAb, demonstrating their GD_2 expression. Hence, NKL, RL12, M21 and NXS2 cells all bind the hu14.18-IL2 IC (Fig. 1A,B). These findings suggest that hu14.18-IL2 IC binds to these NK cells via the high affinity form of IL2R containing CD25, and to tumor cells via GD_2. CD25-specificity of hu14.18-IL2 IC was confirmed by separate analyses where IC binding to NKL and RL12 cells was inhibited by pre-incubating them with anti-CD25 (anti-TAC) mAb (see Figs. 4A, 4B and 5 in Gubbels et al companion study[3]). Furthermore, the binding of the hu14.18 mAb to GD_2^+ tumor cells but not to $CD25^+$ NKL or RL12 cells further confirms that hu14.18-IL2 IC binds to NKL and RL12 via CD25. Cells that do not express GD_2, CD16 or CD25 (K562, Fig. 1B*i*, and CT26, Fig. 1B*ii*) do not bind hu14.18 mAb or hu14.18-IL2 IC. The amount of hu14.18-IL2 IC (and hu14.18 mAb) bound to the cells correlated with the level of CD25 and GD_2 expression (Fig. 1B). L5178Y cells, expressing the highest level of CD25 shown (Fig. 1B*i*) bound more hu14.18-IL2 IC than did NKL or RL12 cells. Similarly, M21 cells, expressing more GD_2 than NXS2 cells bound more hu14.18-IL2 IC than did NXS2

cells (Fig. 1B*ii*). The binding of hu14.18-IL2 to NK cells expressing only the intermediate form of the IL-2R [i.e. unstimulated human donor peripheral blood mononuclear cells (PBMC)-derived NK cells] was not studied. However, in a parallel study (Figs 1 and 2 in Gubbels et al[3]) it has been demonstrated that another immunocytokine, KS-IL2 IC can effectively facilitate conjugate formation between ovarian cancer cells and NK cells derived from PBMC of healthy donors and ovarian cancer patients. Since most NK cells (both PBMC derived and human NK cell lines growing in vitro) express at least low levels of the intermediate affinity receptor, and proliferate in response to IL-2, it is possible that the amount of hu14.18-IL2 binding to CD122 needed to induce proliferation may be too small to detect using the flow cytometric methods employed in this study.

As levels of CD25 expression can be modulated by exposure to exogenous IL2 [34], we next tested if different cell culture conditions would affect the level of hu14.18-IL2 IC binding to NKL and RL12 cells (Fig. 1C). NKL and RL12 cells, grown under our standard *in vitro* conditions in medium supplemented with 25 U/ml of IL2, were either grown for 7 days in the presence of high IL2 concentration (200 U/ml) or were IL2 deprived for 24 hr prior to testing for CD16/CD25 expression and hu14.18-IL2 IC binding. As shown, culturing in the presence of 200 U/ml of IL2 upregulated CD25 expression on NK cells as well as augmented the capacity to bind hu14.18-IL2 IC, whereas IL2 deprivation led to down-regulated CD25 expression and decreased IC binding, especially for RL12 cells (Fig 1C).

Hu14.18-IL2 IC facilitates conjugation of NK with GD_2^+ tumor cells resulting in tumor cell lysis

We have recently found that hu14.18-IL2 IC facilitates the conjugation of fresh PMBC-derived

NK cells to GD_2^+ tumor cells, and that these conjugates exhibited a polarized immune synapse facilitated by the IL2Rs of the effector cells (J.A.A.G, data not shown). Here we tested the cytotolytic activity of these IC-facilitated conjugates. We first confirmed that hu14.18-IL2 IC facilitated conjugate formation between NKL and GD_2^+ M21 cells (Fig. 2A) and demonstrated that a similar result is obtained with the RL12 cells (Fig. 2B). In medium alone, only ~2% of the mixed cells were engaged in formation of conjugates that involved at least one tumor cell and one NK cell (upper right quadrant on each histogram in Fig. 2A and 2B). Incubating the cells in the presence of hu14.18 mAb or IL2, alone or in combination, did not significantly increase the number of cells forming hetero-conjugates. In contrast, the presence of hu14.18-IL2 IC led to formation of conjugates (involving 17-22% of the events detected by flow cytometry) within the first 30 min of incubation (Fig. 2). Addition of exogenous IL2, similarly to the control setting of hu14.18 mAb + IL2, at 3000 U/ml did not visibly interfere with the process of functional conjugation facilitated by hu14.18-IL2 IC. Separate analyses have shown these conjugates are mediated through the high affinity IL2Rs of the effector cells as anti-CD25 (anti-TAC) mAb dramatically inhibits conjugate formation (Figs 4B, 4C and 5 in Gubbels et al[3]). When NKL or RL12 cells were tested for conjugate formation with GD_2^- K562 cells, no significant differences between hu14.18 mAb and hu14.18-IL2 IC were observed, with only 3-5% of the cells forming conjugates (I.N.B., data not shown). Figure 2C (***i***, M21+NKL and ***ii***, M21+RL12) summarizes results of 3 experiments performed under identical conditions.

Mixing NKL effectors with M21 targets in the presence of IC at a 1:1 E:T ratio led to formation of conjugates between ~28% of mixed NKL and M21 cells (Fig. 3B) and involving 45% (Fig. 3C) of total M21 cells during the first 30 min of the assay. We asked if increasing the E:T ratio would increase the percentage of M21 cells that were conjugated with effector cells. At the

3.75:1 E:T ratio more than 80% of the M21 cells were bound to NKL cells (Fig 3B, C), and 90% of the M21 cells were bound to NKL cells at the 7.5:1 E:T ratio. At the ratios of 15:1 and 30:1 greater than 95% and 99% of M21 cells, respectively, were conjugated to NKL cells (Fig 3C). Similar results were found with RL12 cells (data not shown). In contrast, the percentage of M21 cells involved in conjugates in the presence of hu14.18 mAb was less than 16%, even at the 15:1 and 30:1 E/T ratios (Fig. 3A, C).

In next series of experiments NKL (Fig. 4A*i*,*iii*) and RL12 (Fig. 4A*ii*,*iv*) cells were tested for killing of the GD_2^+ M21 (Fig. 4A*i*,*ii*) and the GD_2^- K562 (Fig. 4A*iii*,*iv*) cells. Greater cytotoxicity was mediated against M21 cells in the presence of hu14.18-IL2 IC as compared to hu14.18 mAb. Adding equivalent amounts of IL2 with hu14.18 mAb did not enhance target lysis. In contrast, comparable killing was seen on K562, regardless of whether hu14.18-IL2 or hu14.18 mAb + IL2 was added. M21 tumor cell lysis was markedly inhibited when effector cells, NKL (Fig. 4B*i*) or RL12 (Fig. 4B*ii*), were pre-coated with anti-CD25 (anti-TAC) mAb prior to being admixed with the M21 tumor cells. This is consistent with the results shown in Fig. 5 of the companion study by Gubbels et al.[3], and suggests that conjugation of NK cell effectors with tumor cell targets facilitated by mAb-IL2 IC augmented cytotoxicity and requires interaction of IC and the IL2R present on effectors.

Differential stability of hu14.18-IL2 IC binding to GD_2^- $CD25^+$ NK cells and GD_2^+ $CD25^-$ tumor cells reflects differential IC internalization

The half-life of high-affinity IL2R expression on the cell surface is approximately 10-20 minutes [18, 20]. Shortly after IL2 binding, the IL2-IL2R complex becomes internalized, and this process seems to be independent from the presence of IL2 in the microenvironment but rather depends

upon temperature [19]. The IL2 molecule, as well as β- and γ-chains of IL2R are then degraded, whereas the α-chain (CD25) is recycled to the cell surface. At 37^0C more than 50% of IL2 bound to high affinity IL2Rs becomes internalized within the first 10-20 minutes, and more than 80% - by one hour [18-20, 35].

Similarly, monoclonal antibodies that recognize membrane surface antigens, can either be internalized, or shed, or remain relatively stable on the cell surface. This process is also temperature and cell type dependent and is affected by character and membrane location of the antigen as well as the class of monoclonal antibody recognizing it. As the gangliosides expressed by tumor cells are relatively stable membrane components, antibodies that bind to them may remain on the cell surface for a longer period of time, with slow shedding or internalization [26, 27].

Because hu14.18-IL2 IC is a bispecific fusion protein that binds to both the GD_2 and IL2Rs (Fig. 1), the fate of the IC once bound to either GD_2^+ M21 cells or NK cells was investigated (Figure 5). We hypothesized that at least three potential possibilities could occur: A*i*) hu14.18-IL2 IC internalization, A***ii***) stable binding of IC, or A***iii***) loss of surface-bound IC via shedding without internalization.

To address this hypothesis, we used FITC-labeled hu14.18-IL2 IC (IC-FITC) as well as APC-labeled secondary polyclonal goat anti-human IgG antibody (IgG-APC) that would specifically recognize human IgG (IC) but not other proteins. M21, NKL and RL12 cells were pre-armed on ice with saturating concentrations of FITC-labeled hu14.18-IL2 IC and excess IC was washed out. The amount of IC present on the cell surface at this time (time point 0 hr) should correspond to 100% of the IC bound to the cell. Thus the amount of IC-FITC detected on the cell surface by FITC detection, and the amount of IC on the cell surface detected by the secondary anti-human

IgG-APC reagent, at time = 0 were defined as 100% for both FITC and APC.

In the case of IC-FITC internalization, FITC would presumably be retained in the cells (but not on the surface) without significant FITC metabolism and quenching [36]. If all of the IC were internalized, the amount of human IgG (IC-FITC) available on the cell surface for recognition by the anti-IgG-APC, would become absent, resulting in reduction of APC fluorescence of the cells with internalized IC-FITC. A diagram showing the hypothetical pattern for the anticipated FITC/APC fluorescence decline under the circumstances of complete hu14.18-IL2 IC internalization is shown in Fig. 5A*i*. Previously published data on the kinetics of IL2-IL2R complex internalization [18, 20] were used as a model.

In the hypothetical case of complete stable binding of hu14.18-IL2 IC to the cell surface (no shedding or internalization), most of the cell surface bound IC-FITC would still be available for detection with anti-IgG-APC and thus no decline in either FITC or APC fluorescence would be anticipated. A diagram showing this pattern for the anticipated FITC/APC fluorescence is presented in Fig. 5A*ii*. Should all of the cell surface-bound IC-FITC be shed, there would be a reduction of FITC fluorescence. Since less IC-FITC would be available for recognition with IgG-APC, the APC fluorescence will also decrease. This hypothetical pattern is presented in Fig. 5A*iii*.

First we tested our hypothesis by comparing FITC and APC fluorescence of NKL (Fig. 5B*i*,*ii*) and M21 (Fig. 5B*iii*,*iv*) cells at 0 and 24 hours after pre-arming the cells with hu14.18-IL2 IC. Both NKL and M21 cells retained 75-85% of FITC fluorescence after being in culture for 24 hr, indicating that most of the FITC labeled hu14.18-IL2 had been retained on the surface or internalized, rather than being shed. In contrast, the anti-human IgG-APC fluorescence of NKL cells had diminished dramatically (from 330 MFI at 0 h to 12 MFI at 24 h), indicating that most

of surface-bound IC-FITC had been internalized. At 24 h, the M21 cells still retained most of their IgG-APC signal (2340 MFI at 0 h and 1588 MFI at 24 h), indicating that most of their IC-FITC was retained on the surface.

Next we evaluated the kinetics of IC cell surface-retention and internalization for IL2-dependent $GD_2^-CD25^+$ NKL (Fig. 5C*i*,*iv*) and RL12 (Fig. 5C*ii*,*v*) NK cells, and IL2-independent GD_2^- $CD25^+$ L5178Y T lymphoma cells (Fig. 5C*iii*,*vi*) and for two $CD25^-GD_2^+$ tumor cell lines M21 and NXS2 (Fig. 5C*iii*,*vi*), based on analysis of reduction of FITC (Fig. 5C*i-iii*) and APC (Fig. 5C*iv-vi*) signals. We additionally tested if modulations in the growth conditions of NK cells (increased IL2 concentration in medium or IL2-deprivation, as shown in Fig. 1C) have an impact on the stability of hu14.18-IL2 IC binding to the cell surface. Even though NKL and RL12 cells grown in the presence of high concentrations of IL2 (200 U/ml) bind more IC at time 0 h (Fig. 1C), we observed no significant difference in the rate of hu14.18-IL2 IC internalization by these cells as compared to the cells propagated in standard (25 U/ml) IL2 concentrations: at 6 hr IC-FITC fluorescence was almost unchanged from the levels detected at time point 0 hr, whereas anti-IgG-APC fluorescence declined by 60-75% at 6 h. Likewise, no significant difference in the kinetics of hu14.18-IL2 IC internalization was found when cells were deprived of IL2 prior to pre-arming with IC, although a reduction of the amount of IC bound to the cells at 0 h was noted and likely reflected down-regulation of CD25 expression. Similar results were documented for NKL (Fig. 5C*i*,*iv*) and RL12 (Fig. 5C*ii*,*v*) cells. The IL2-dependence status [IL2-independent $CD25^+$L5178Y (Fig. 5C*iii*,*vi*) cells vs. IL2-dependent $CD25^+$NKL (Fig. 4C*i*,*iv*) and $CD25^+$RL12 cells (Fig. 5C*ii*,*v*)] also had no detectable impact on the kinetics of hu14.18-IL2 IC internalization; the pattern seen for L5178Y is very similar to that seen for NKL and RL12. In contrast, both $CD25^-GD_2^+$ tumor cells, M21 and NXS2 (Fig. 5C*iii*,*vi*) lost less than 30% of their

surface-bound hu14.18-IL2 IC over the 24 hr culture at 37^0C (as measured by APC fluorescence). Hence, it appears that both effectors and targets can internalize the surface-bound IC when incubated at 37^0C, but this effect is mediated more rapidly via IL2Rs than by GD_2.

Internalization of IC by NK cells modulates their effector function

To test if internalization of surface-bound hu14.18-IL2 IC had an effect on the ability of IC-armed cells (effectors or targets) to form conjugates (Fig 6), either NKL cells (Fig. 6*iv*) or M21 cells (Fig. 6*iii*) were pre-armed with hu14.18-IL2 IC, washed and cultured for 1, 6 or 24 hr prior to being tested in the conjugate formation assay. As a control, cells were allowed to form conjugates in the continued presence of either hu14.18 mAb (Fig. 6*i*) or hu14.18-IL2 IC (Fig. 6*ii*) or immediately after (i.e. at time point 0 hr) the cells were pre-armed with hu14.18-IL2 IC. As expected, NKL and M21 cells formed more conjugates in the continuous presence of IC but not mAb (Fig. 6*i*, *ii*). Although we found a slight reduction in the amount of IC on the surface of M21 cells over time while incubated at 37^0C, this did not affect their ability to become engaged with IC-unarmed NKL cells (Fig. 6*iii*) as the percentage of conjugates formed with M21 cells 24 hr after pre-arming was almost the same as for the cells that were pre-armed 0, 1 and 6 hr before the assay. In contrast, NKL cells pre-armed with IC formed fewer conjugates even at time 0 than the pre-armed M21 cells (Fig.6*iv* vs. Fig. 6*iii* at 0 h), likely reflecting the lower amount of IC that binds to NKL as compared to M21 (Fig. 1A and Fig. 4B). After the pre-armed NKL were incubated at 37^0C for 1, 6 or 24 h, further decreases were seen in their ability to form conjugates; at the 24 hr time point the % of conjugates was similar to the number of conjugates formed in the presence of hu14.18 mAb (7.7% vs. 5.6%, respectively). Hence, rapid internalization of hu14.18-IL2 IC by pre-armed NK cells (Fig. 5C***i***,***ii***,***iv***,***v***) can diminish their ability to subsequently link to

tumor cells, whereas pre-armed tumor cells can still be effectively targeted by NK cells even 24 hr after IC binding to the tumor cell surface.

To test if internalization of IC by pre-armed NK cells impacts the hu14.18-IL2 IC-facilitated cytotoxicity, pre-armed NKL (Fig. 7A***i***,***ii***) and RL12 (Fig. 7A***iii***,***iv***) cells were tested for lysis of GD_2^+M21 (Fig. 7A***i***,***iii***) or GD_2^-K562 (Fig. 7A***ii***,***iv***) cells at different time points after IC-arming. The results suggest that immediately after the arming (0 h) both NKL and RL12 cells could effectively lyse M21 cells at a level similar to that observed when hu14.18-IL2 IC was continuously present in the medium. The cytotoxicity levels were reduced at all E/T ratios by ~50% and ~75% at the 6 hr and 24hr time-points, respectively (Fig. 7A*i*,*iii*). Full recovery of cytotoxicity by the 24 hr IC–pre-armed NKL (or RL12) cells could be achieved if 1 μg/ml of exogenous hu14.18-IL2 IC was added to the culture (I.N.B., data not shown). As noted in Fig. 3, no augmented cytotoxicity against K562 cells by IC-armed NK cells was mediated (Fig. 7A*ii*,*iv*). In contrast to the pre-armed NK cells, IC-armed M21 cells were efficiently lysed by unarmed NKL (Fig. 7B*i*) and RL12 (Fig. 7B*ii*) cells at any of the time points after the arming regardless of the loss of some of the hu14.18-IL2 IC from the cell surface (Fig. 5C*iii*,*vi*). These results are consistent with the results shown in Fig. 6*iii* where efficient conjugate formation at all time-points was documented. While the level of cytotoxicity seen in Figs. 7A*ii* and 7A*iv* on K562 appears enhanced by IC and likely reflects NK stimulation by the IL2-component of IC, this was not always reproducible; in 4 separate experiments (not shown) this difference was not significant ($p>0.10$).

Hu14.18-IL2 IC preferentially binds to targets in a mixture of tumor and NK cells

Hu14.18-IL2 IC effectively mediates conjugation of tumor cells with NK cells when

continuously present in medium (Fig. 2), even though the MFI of IC binding to NK cells is less than to tumor cells (Fig. 1) and IC is internalized more rapidly by NK cells than by tumor cells (Fig 5). To potentially simulate the *in vivo* setting of IC administration, we tested the binding of hu14.18-IL2 IC to a mixture of un-armed M21 tumor cells and NK cells at 37^0C.

$1.5x10^5$ NKL (Fig. 8A*i*, blue population) and $1.5x10^5$ M21 cells (Fig. 8A*i*, red population) were mixed in a 1:1 E:T ratio in the presence of 1 μg/ml of hu14.18 mAb (Fig. 8A*ii*,*v*) or hu14.18-IL2 IC (Fig. 8A*iii*,*vi*) and conjugates (Fig. 8A*ii*,*iii*,*v*,*vi*, green population) were allowed to form at 37^0C for 30 min. Cell surface-bound hu14.18 mAb and IC were detected with anti-human IgG mAb similar to the strategy in Fig. 5 (Fig. 8A*iv*-*vi*). Cells kept in medium alone (no mAb or IC) were used as a control (Fig. 8A*iv*). Distribution of hu14.18 mAb and hu14.18-IL2 IC on single, i.e. unconjugated cells (red – M21, blue – NKL) as well as on M21/NKL conjugates (green) is shown in Fig. 8A*v*,*vi*. We found that both hu14.18 mAb and hu14.18-IL2 IC were bound to unconjugated M21 cells (Fig. 8Av,*vi*). The hu14.18-IL2 IC was also bound to M21/NKL cell conjugates (Fig. 8A*vi*). NKL cells were stained negatively for hu14.18 mAb (Fig. 8A*v*) and only weakly positive for hu14.18-IL2 IC (Fig. 8A*vi*).

To further address the relative binding of mAb vs. IC to the mixed M21 and NKL cells, we titrated concentrations of hu14.18-IL2 IC to ascertain that the IC concentration of 1 μg/ml was not a major limiting factor for the low binding of IC to the population of unconjugated NKL cells. At both low (0.25 μg/ml) and high (4 μg/ml) hu14.18-IL2 IC concentrations, IC staining is far more prominent on unconjugated M21 cells (Fig. 8B, white triangles) and on M21/NKL cell conjugates (Fig. 8B, black squares), with smaller levels of IC present on unconjugated NKL cells (Fig. 8B, black circles).

Intratumoral hu14.18-IL2 IC treatment results in migration of NK cells into the tumor.

It was previously shown that systemic [i.e. intravenous (IV)] treatment with hu14.18-IL2 IC results in pronounced antitumor effects against mouse NXS2 NB [13], with even greater local and systemic effects obtained when the IC is delivered IT [16]. However, little is known about the ability of such IT treatment to facilitate migration of NK cells into the tumor. We evaluated this using a previously described adoptive transfer xenograft model [37].

C.B17/SCID mice bearing subcutaneous human M21 melanoma tumors received either one or three IT injections of 10 μg hu14.18-IL2 IC. To control for mechanic factors associated with IT injections, mice from the control group received 3 IT injections of 50 μl PBS. Immediately after the last PBS or IC treatment, all mice were adoptively transferred with $5x10^6$ BODIPY-labeled NKL cells by IV injection. Twenty four hr after NKL cell infusion the tumors were harvested, processed into single cell suspension and evaluated for the presence of endogenous mouse $CD49B^+$ NK cells as well as the presence of $BODIPY^+$ NKL cells. A representative sample from a mouse that received 3 daily IC treatments is shown in Fig. 9A. A summary of NK/NKL cell prevalence in the tumors from all mice in each of the three treatment groups is shown in Fig. 9B. The results suggest that even a single IT injection of hu14.18-IL2 IC induced migration of both resident and adoptively transferred human NK cells into the tumor, and the effect of three IT IC treatments was greater than that of a single treatment (Fig. 9B). A single IT IC treatment was also marginally better at induction of NKL cell migration than a single IV treatment with the same amount of IC (I.N.B., preliminary data not shown).

We also asked whether IC was still present in the tumor 24 hr after the last IT treatment and on which cells it might be bound. The single cell samples from the harvested tumors were labeled with secondary PE-conjugated polyclonal goat anti-human IgG antibody as well as with FITC-

conjugated anti-murine NK mAb (anti-CD49B-FITC). The cells were analyzed for IC binding (PE staining) by gating on CD49B-FITC^{+} (murine NK cells), on BODIPY^{+}(human NK cells) or on FITC^{-}BODIPY^{-} cells (murine tumor and non-NK stromal cells) of the samples (Fig. 8A). We found that IC was detectable on the surface of FITC^{-}BODIPY^{-} cells (M21 tumor cells + non-NK stroma) and was not detectable on the surface of either mouse resident CD49B^{+}NK cells or injected BODIPY^{+} human NK cells (Fig 9C). The number of IC treatments (1 vs. 3) did not have a visible effect on the amount of IC present on FITC^{-}BODIPY^{-} cells (Fig. 9C).

Discussion

In this study we evaluated the stability of binding of IC to $GD_2^+CD25^-CD16^-$ tumor cells and $CD25^+GD_2^-CD16^-$ NK cells, and evaluated *in vitro* the impact of IC internalization on the effector-to-target conjugation and cytotoxicity processes. NK cells were found to rapidly internalize IC similar to that previously described for soluble IL2; this internalization did not depend on the amount of IC bound to the NK cell surface (Fig. 1B*i,ii*, and Fig. 5C*i,ii,iv,v*), the concentration of exogenous IL2 (Fig. 1C., and Fig. 5C*i,ii,iv,v*) in the microenvironment or overall IL2-dependance of the $CD25^+$ cells (Fig. 5C). Loss of IC from the cell surface of pre-armed NK cells resulted in a significant reduction in their capacity to form conjugates with (Fig. 6*iv*) and kill (Fig. 7A) tumor cells. However, these functions were easily recovered by supplying additional hu14.18-IL2 into the mixed M21/NKL cell cultures (I.N.B., not shown). While the effector cells evaluated here (NKL and RL12) express the high-affinity IL2R (αβγ), it is possible that the kinetics of IC internalization by effectors expressing only intermediate-affinity IL2R (βγ) may be different. Furthermore, concomitant CD16 expression by NK cells may substantially alter the process of internalization and cytotoxicity by enabling further binding of IC to the cell surface of effectors and by providing additional stimuli via activating FcγRIII. However, it appears that IC-facilitated cellular cytotoxicity can be mediated by $CD25^+$NK cells that lack expression of CD16, with CD25 serving as both anchoring and stimulatory ligand. In contrast, the kinetics of IC internalization by GD_2-positive tumor cells was considerably slower (Fig. 5C), as compared to NK cells; the stable surface binding of IC to these tumor cells allowed for efficient conjugation of IC-armed $GD2^+$ tumor cells to IC-unarmed NK cells (Fig. 6*iii*), and resulted in efficient tumor cell lysis (Fig. 7B).

While the binding of hu14.18-IL2 IC to M21 cells is mediated by the IC's GD_2-specific tumor

antigen recognition mAb component, the ability of IC to facilitate effector-to-target conjugate formation and tumor cell lysis (particularly by $CD25^+CD16^-$ effectors) reflects the bispecific design of the IC molecule, and its IL2 components. Similar functional results, showing enhanced NKL-tumor cell conjugation, were recently demonstrated using a separate IC, the huKS-IL2 IC (Gubbels et al.[3]) that specifically targets the KS1/4 [epithelial cell adhesion molecule (EpCAM)] antigen expressed on lung [38], ovarian [39], colon and other adenocarcinomas [40]. Conjugate formation between $GD2^+$M21 cells or KS^+OVCAR ovarian carcinoma cells and $CD25^+$NK effectors (NKL or RL12 cells), facilitated by hu14.18-IL2 IC or huKS-IL2 IC, respectively, was markedly inhibited by pre-treating NK cells with anti-CD25 (anti-TAC) mAb (Gubbels et al.[3]). IC target-specificity was shown by the absence of effector-tumor conjugate formation between NKL and M21 ($GD_2^+EpCAM^-$) cells in the presence of saturating concentrations of huKS-IL2 IC (Gubbels et al.[3]). Most importantly, within the NKL-tumor cell conjugates, the IC bound to the surface of the tumor cells remained evenly distributed all over the tumor cell surface, while the IC and CD25 molecules on the surface of the NKL cells co-polarized to the active immune synapse at the junction of the NKL and tumor cell (Gubbels et al.[3]). These studies indicate that the high affinity IL2R, upon encountering cell-bound IL2 (as IC bound to tumor cell), functions as a potential adhesion molecule as well as a signaling molecule, and participates in activated immune synapse formation. Prospective studies with human NK cells, both resting and IL2-activated, will address the conjugate formation, cytotoxicity and cytokine profile of patient effectors *ex vivo*.

Despite ostensibly uniform binding of IC to NK and M21 cells within a sample (Fig. 1A), it was never possible to achieve 100% conjugation of all tumor cells with all NK cells when the cells were mixed at 1:1 E:T ratio (Fig. 2, Fig 3). However, shifting the E:T ratio in favor of NK cells

(Fig. 3) results in a greater percentage of the tumor cells becoming conjugated with the NK cells. This greater percentage of conjugation at higher E:T ratios is paralleled by better cytotoxicity (Fig. 4A). When E:T ratios were less than 1:1 (i.e., more tumor cells compared to effectors), only a fraction of tumor targets were conjugated with NK cells and resulted in diminished cytotoxicity (I.N.B, data not shown). Many biological factors, such as overall density and character of surface distribution of additional adhesion receptor-ligand pairs on both effectors and targets (i.e: NK activating receptors, such as NKG2D, and its ligands), size of the cells, etc., may have a functional impact on the quantitative equilibrium of conjugation between the NK and tumor cells. Regardless of which effector line was evaluated in this study, the inclusion of the hu14.18-IL2 IC (versus IL2 alone, hu14.18 mAb alone or the IL2 and mAb together) unequivocally resulted in the highest level of conjugation formation between NKL or RL12 cells and the GD_2^+ tumor cells (Fig. 2).

Another aspect of IC biology was revealed by comparing the amount of IC bound to single M21 or NKL cells, or to conjugated M21/NKL cells, after 30 min of mixed cell pellet incubation at 37^0C (Fig. 8). Cell-bound IC was predominantly targeted to tumor cells (Fig. 8A*vi*, red cell population), rendering them vulnerable to killing by NK cells. In contrast, NK cells (Fig. 8A*vi*, blue cell population) had a much smaller amount of IC on their surface. NKL/M21 cell conjugates (Fig. 8A*vi*, green cell population) contained IC at a level comparable to the levels observed on unconjugated M21 cells. Increasing the concentration of IC in the culture medium (Fig. 8B) did not significantly alter the pattern of IC binding to the cells in the cell mixture, with M21 cells always demonstrating significantly greater binding of IC relative to NKL cells. While this may reflect the greater cell-surface density of GD_2 antigen on M21 as compared to that of high affinity IL2Rs on the NK effectors, it is also possible that most IC bound to NKL cells at

37^0C is rapidly internalized (Fig. 5) and no longer detectable.

As a potential *in vivo* correlate of our *in vitro* binding studies, we demonstrated that intratumoral injections of hu14.18-IL2 IC in SCID mice resulted in augmented recruitment of NK cells into the tumor (Fig. 9A,B). In several preliminary experiments, we did not detect significant influx of NK cells into the tumor when IC was administered intravenously; this likely reflects the non-optimized conditions employed. The number of adoptively transferred human NKL cells found in the tumor was greater for the animals receiving 3 daily IT injections than a single IT dose of IC. This effect required IC treatment, as injections of PBS in control animals did not induce active migration or passive extravasation (due to mechanical disturbance of the tumor) of either resident mouse $CD49B^+$NK cells or adoptively transferred human $BODIPY^+$ NKL cells. Interestingly, when the single cell preparations from the harvested tumors were tested for the presence of IC on the cell surface, the IC was found only on tumor cells but not on NK cells (Fig. 9C). It is possible that the tumor-infiltrating NK cells have rapidly internalized any IC bound to them after IT treatment, whereas the slower internalization kinetics of IC on the surface of tumor cells enabled its detection at the time of tissue harvest. It is unlikely that this increased number of NK cells in the tumors was due to immunotherapy-induced tumor cytoreduction, as decreased tumor sizes was not observed during the 96 hr of the experiment (I.N.B., data not shown). However, we anticipate that continued (i.e. beyond 96 hr) therapy with the combination of adoptively transferred NK effectors plus IT delivery of IC would result in even greater accumulation of NK cells in the tumor compartment leading to immunotherapy-induced tumor cytoreduction.

The phenomena of differential internalization and surface labeling of tumor vs. effector cells with IC may have some practical implications in the setting of *in vivo* treatment, and may

potentially relate to antitumor activity seen recently in the Phase II clinical setting [43]. In our preliminary experiments we found that IC bound to the surface of pre-armed NKL cells did not facilitate their migration into the tumor once the IC-armed NKL cells were adoptively transferred into the systemic circulation of M21 tumor-bearing mice (I.N.B., data not shown), possibly due to rapid IC internalization prior to NK cells reaching the tumor. In contrast, IT therapy with IC did facilitate recruitment of NK cells into the tumor compartment. Prior studies with radio-labeled IC show specific *in vivo* localization to tumor sites after IV injection of IC, with even greater amounts of IC localization to tumor sites after direct IT administration [16]. Despite the relatively short half-life of IC in the circulation after IV injection [10,41,42], the studies presented here suggest that once the IC gets to the tumor cells *in vivo*, it would appear to remain there for some time. The IC that remains on the tumor surface would then facilitate conjugate formation with NK effectors that express IL2Rs, subsequently resulting in IC-mediated cytotoxicity.

Figure legends

Figure 1. Binding of hu14.18-IL2 IC and hu14.18 mAb is determined by pattern of CD16, CD25 and GD_2 expression on NK cells and tumor cells. ***A.*** Expression of CD16 (grey open peaks) and CD25 (grey filled peaks) vs. staining with isotype IgG (black filled peaks) on NKL cells (***i***) and M21 cells (***iii***). Binding of hu14.18 mAb (grey open peaks) and hu14.18-IL2 IC (grey filled peaks) or isotype IgG (black filled peaks) to NKL cells (***ii***) or M21 cells (***iv***). Numbers represent geometric mean values of the mean fluorescent intensity (MFI) of the staining with specific or control IgG Ab. ***B***. Comparison of binding by anti-CD16, anti-CD25, hu14.18 mAb or hu14.18-IL2 IC to NKL, RL12, L5178Y or K562 cells (***i***), or M21, NXS2 or CT26 cells (***ii***). Results are presented as Mean ± SE (n = 4 independent experiments with similar design) of MFI ratios calculated by using geometric mean values of the MFI as described in Materials and Methods. * - $p < 0.05$; # - $p > 0.05$ ***C***. Comparison of binding by anti-CD16, anti-CD25, hu14.18 mAb or hu14.18-IL2 IC to NKL or RL12 cells grown in 25 U IL2/ml, deprived of IL2 for 24 h, or cultured in 200 u/ml for 7d prior to staining. Results are presented as MFI ratios. Results are presented as Mean ± SE (n = 3 independent experiments with similar design) of MFI ratios calculated by using geometric mean values of the MFI as described in Materials and Methods. * - $p < 0.05$; # - $p > 0.05$

Figure 2. ***A, B.*** **IC facilitates conjugation of NK and tumor cells** ***in vitro*****.** BODIPY 630/650-labeled M21 cells ($1.5x10^5$/0.1 ml) and CFSE-labeled NKL (***A***, $1.5x10^5$/0.1 ml) or RL12 (***B***, 1.5x105/0.1) cells were mixed together in sample tubes in complete RPMI-1640 medium with or without 1 μg/ml hu14.18 mAb, 3000 U/ml rIL2, 1 μg/ml hu14.18 mAb + 3000 U/ml rIL2, 1 μg/ml hu14.18-IL2 IC or 1 μg/ml hu14.18-IL2 IC+ 3000 U/ml rIL2, and a loose pellet was formed by centrifugation at 500 rpm/1 min followed by incubation of the pelleted cells for 30

min on a 37°C water bath. After 30 min of incubation the pellet was gently agitated and the cells were tested by flow cytometry for M21-NK cell conjugate formation. The numbers in each quadrant indicate the percentage of events: single NK cells (left upper quadrant), single M21 cells (right lower quadrant) and conjugates containing at least 1 M21 cell and 1 NK cell (right upper quadrant). ***C***. Summary of NKL (C***i***) and RL12 (C***ii***) effector cells plus M21 tumor cell conjugate formation experiments (n = 3). The assays were performed as described above and in Materials and Methods section. Results are presented as Mean ± SE of percentage total number of cells, mixed in 1:1 E/T ratio, involved in conjugates, as opposed to single cells, by using geometric mean values of the MFI. * - $p < 0.05$; # - $p > 0.05$

Figure 3. Increasing E:T ratio increases percentage of M21 cells in conjugates.

NKL cells (1.5 x 10^5/0.1 ml) were mixed with 1.5, 0.4, 0.2, 1 or 0.050 x 10^5/0.1 ml M21 cells to achieve E:T ratios of 1:1, 3.75:1, 7.5:1 (**A,B**), 15:1 or 30:1 (**C**, and not shown in **A**, **B**) ratios. These mixtures were cultured in medium with 1 µg/ml of hu14.18 mAb (**A**) or hu14.18-IL2 IC (**B**), and conjugates were allowed to form at 37^{0}C. After 30 min of incubation the pellets were gently re-suspended and tested by flow cytometry for M21-NK cell conjugate formation. Conjugates were scored as in Figure 2. **C.** For the purpose of calculating the distribution of M21 cells that were conjugated to NKL cells, versus free (unconjugated) M21 cells, the following calculations assume that each event seen by flow cytometry represents either a single M21 cell, a single NKL cell, or a conjugate consisting of 1 M21 and 1 NKL cell. However, it remains possible that some of the events detected by flow (particularly in the right upper quadrant) may have more than a single M21 or single NKL cell. The percentage of M21 cells in conjugates = 100% - [(***x***/***y***) x 100%] where ***x*** is absolute number of unbound M21 cells calculated from the percentage of events in lower right quadrants in **A** and **B**, and ***y*** is the absolute number of total

M21 cells mixed with NKL cells prior to adding hu14.18 mAb or hu14.18-IL2 IC. The results are representative of two independent experiments.

Figure 4. IC facilitates NK-mediated cytotoxicity *in vitro*. NKL (**A*i,iii***) or RL12 (**A*ii,iv***) cells, grown in medium supplemented with 25 U/ml of IL2, were tested for cytotoxicity against $5x10^3$ M21 (***i***,***ii***) or K562 (***iii***,***iv***) in the presence of 1 μg/ml hu14.18 mAb, 3000 U/ml rIL2, 1 μg/ml hu14.18 mAb + 3000 U/ml IL2, or 1 μg/ml hu14.18-IL2 IC, as described in Materials and Methods section. Results are presented as % cytotoxicity mediated at different E:T ratios, and are representative of at least two independent experiments. **B**. NKL (**B*i***) or RL12 (**B*ii***) cells were tested for cytotoxocity against $5x10^3$ M21 cells in the presence of 1 μg/ml hu14.18 mAb or 1 μg/ml hu14.18 mAb + 3000 U/ml IL2 after some NKL and RL12 cells had been pre-coated with excess (10 μg/ml) of anti-CD25 (anti-TAC) mAb for 1 hr. This experiment was performed one time.

Figure 5. Kinetics of hu14.18-IL2 IC internalization by GD_2^+ tumor cells and $CD25^+$ lymphoid cells. *A.* Three alternative possible patterns for the anticipated retention (%) of FITC (bound to hu14.18-IL2 IC) or APC (bound to secondary goat antibody against human IgG) in the hypothetical case of complete internalization (***i***), complete stable surface binding (***ii***) and complete loss due to shedding (***iii***) over a 24 hour period for the hu14.18-IL2 IC bound to the surface of CD25+ cells. Previously published data on analysis of IL2R internalization were used to generate these 3 hypothetical plots. ***B.*** Hu14.18-IL2 IC-FITC – armed NKL (***i***, ***ii***) or M21 (***iii***, ***iv***) cells ($3x10^6$/0.1 ml) were cultured for 0-24 hr at 37^0C. After 0-24 hr, the cells were labeled with goat anti-human IgG-APC to detect any IC-FITC still present on the surface. The double-labeled cells were analyzed by flow cytometry for both FITC (***i***, ***iii***) and APC (***ii, iv***). The numbers shown are MFI geometric mean values at 0 hr (black open peaks) or 24 hr (grey filled

peaks). Black filled peaks demonstrate the FITC signal from control IgG-FITC (rather than IC-FITC) (***i***, ***iii***) or the APC signal from the IgG-FITC labeled cells developed with goat anti-human IgG-APC (***ii***, ***iv***). ***C.*** Comparison of time-dependent alterations of FITC (***i-iii***) and APC (***iv–vi***) dual fluorescence over 24 hr, for cells pre-armed with hu14.18-IL2-FITC and stained at the indicated times with goat anti-human IgG-APC. NKL (***i***, ***iv***) and RL12 (***ii***, ***v***) NK cells grown in different culture conditions prior to IC-arming (the legend box in panel C***iv*** clarifies the IL2 culture conditions used for the cells shown in ***Ci, ii, iv*** and ***v***). Tumor cells (GD_2^- $CD25^+$ L5178Y T cell lymphoma, GD_2^+ $CD25^-$ M21 and GD_2^+ $CD25^-$ NXS2) are shown in ***iii*** for FITC and in ***vi*** for APC. Results are representative of at least 4 independent experiments, and expressed as % of fluorescence retention at 0.5, 1, 6, 12 and 24 hr (compared to 0 hr = 100%) after IC-arming of the cells. The results are representative of three independent experiments.

Figure 6. IC internalization decreases M21 tumor cell – NK cell conjugate formation. BODIPY630/650-labeled M21 cells and CFSE-labeled NKL cells were tested for conjugate formation 0, 1, 6 or 24 hours after the M21 (***iii***) or NKL (***iv***) cells were pre-armed with hu14.18-IL2 IC and then washed. As a control, M21 and NKL cells were tested for conjugate formation in the continued presence of 1 μg/ml of hu14.18 mAb (***i***) or hu14.18-IL2 IC (***ii***). The figure is representative of four independent experiments with similar results.

Figure 7. IC internalization decreases NK cell mediated M21 tumor cell killing. ***A.*** Hu14.18-IL2 IC – pre-armed NKL (***i***, ***ii***) and RL12 (***iii***, ***iv***) cells were tested for lysis of ^{51}Cr-pulsed M21 (***i***, ***iii***) and K562 (***ii***, ***iv***) cells at 0, 6 and 24 hr after NK cell pre-arming with IC, or in the continued presence of 1μg/ml of hu14.18-IL2 IC (IC in medium). ***B.*** NKL (***i***) or RL12 (***ii***) cells were tested for lysis of IC-armed ^{51}Cr-pulsed M21 melanoma cells at 0, 6 and 24 hr after the M21 tumor cell hu14.18-IL2 IC arming or in the continued presence of 1μg/ml of hu14.18-

IL2 IC. The figure is representative of two independent experiments with similar results.

Figure 8. Binding of IC to GD2$^+$ tumor cells and CD25$^+$ NK cells involved in conjugates vs. those not conjugated. 1.5x10^5 BODIPY-labeled M21 cells (**A*i-vi***, red color population) were mixed with 1.5x10^5 CFSE-labeled NKL cells (**A*i-vi***, blue color population) in 1:1 E:T ratio in medium alone (***i,iv***) or in the presence of 1 μg/ml of hu14.18 mAb (***ii***, ***v***) or 1 μg/ml of hu14.18-IL2 IC (***iii***, ***vi***). The forward and side scatter of the mixed population cultured with medium alone (no mAb or IC) is shown (**A*i***) Conjugates were allowed to form at 37^{o}C for mixtures of NKL and M21 in medium, mAb or IC. After 30 min of incubation, the cell mixtures were washed once with ice-cold PBS and stained with 1 μg/ml of goat anti-human IgG-PE for 40 min on ice. Based on gating for BODIPY and CFSE (**A*ii*** for mAb and **A*iii*** for IC, not shown for medium alone) cells were gated for unconjugated M21 cells (BODIPY$^+$CFSE$^-$, the red population in **A*i-vi***), for unconjugated NKL cells (BODIPY$^-$CFSE$^+$, the blue population in **A*i-vi***), and for conjugates (BODIPY$^+$CFSE$^+$, the green population in **A*ii,iii,v,vi***). These mixtures were then tested by flow cytometry for PE fluorescence (in ***iv, v*** and ***vi***) of the unconjugated M21 cells (red), unconjugated NKL cells (blue) and M21-NKL cell conjugates (green). ***B.*** 1.5x10^5 BODIPY-labeled M21 and 1.5x10^5 CFSE-labeled NKL cells were mixed in 1:1 E:T ratio in the presence of 1 μg/ml of hu14.18 mAb or 0.25-4 μg/ml of hu14.18-IL2 IC for 30 min at 37^{0}C to allow conjugates to form. After 30 min of incubation, the cell mixtures were washed once with ice-cold PBS and stained with 1 μg/ml of goat anti-human IgG-PE for 40 min on ice, and then tested by flow cytometry for PE fluorescence. Results are presented as MFI ratio of PE fluorescence for the unconjugated M21 cells (BODIPY$^+$ CFSE$^-$), for the unconjugated NKL cells (BODIPY$^-$ CFSE$^+$), and for the conjugates themselves (BODIPY$^+$ CFSE$^+$). The figure is representative of two independent experiments with similar results.

Figure 9. IT IC injection facilitates migration of NK cells into the tumor. CB.17/SCID mice (n=12) bearing subcutaneous M21 human melanoma tumors were treated IT with PBS or IC on day 27-29 of tumor growth. Group 1 received 50 µl PBS on days 27, 28 and 29 (PBS x 3); group 2 received 50 µl PBS on days 27 and 28 and 10 µg IC in 50 µl PBS on d 29 (PBS x 2 / IC x 1), group 3 received 10 µg IC on days 27, 28 and 29 (IC x 3). On day 29, immediately after the last injection of PBS (group 1) or IC (groups 2 and 3) all mice were injected IV with $5x10^6$/0.2 ml of BODIPY-labeled NKL cells. On day 30, 24 hr after the NKL cell injection, the tumors were harvested and processed to a single cell suspension. The resultant cell samples from each mouse were counterstained with anti-CD49B-FITC, and samples were tested by flow cytometry for prevalence of mouse resident $CD49B^+$ NK cells and $BODIPY^+$ NKL cells. A representative pattern of staining from a mouse that received 3 days of IT IC (IC X 3) is shown in panel ***A.*** Numbers indicate the relative prevalence (%, Mean ± SEM, n=3) of mouse resident $CD49B^+$ NK cells and implanted $BODIPY^+$ NKL cells of the IC X 3 group. A summary of results for each group of mice is shown in panel ***B.*** Similar results were obtained in two independent experiments. *p=0.06; **p=0.046; @p=0.02; #p=0.007. **C**. The same tumor cell samples shown in **B** were also stained with 1 µg/sample of goat anti-human IgG-PE, which would bind specifically to the IC remaining on the tumor or effector cells, following the *in vivo* IT IC injections (for groups 2 and 3). By gating on FITC or on BODIPY, it was possible to detect the IC bound to mouse resident $CD49B^+$NK cells, to adoptively transferred $BODIPY^+$NKL cells, as well as to the $CD49B^-$/$BODIPY^-$ tumor/stroma cells. MFI of samples from the group that received no IC treatment (group 1) were used as the reference control (defined as MFI-ratio of 1.0). MFI values from the two other experimental groups were compared to the control group. The MFI ratios were calculated by dividing MFI values for each cell subset from groups that

received IC treatment by the MFI value of that same cell subset from the control group that received no IC injections. The results are representative of three independent experiments.

Authorship

I. N. B.: co-primary author, intellectual contributor, study design, data acquisition, data analyses

Z. C. N.: co-primary author, intellectual contributor, study design, data acquisition, data analyses

J. G.: intellectual contributor, study design

T. N. B.: intellectual contributor, study design, data acquisition

M. S. P.: intellectual contributor, study design,

J. A. A. G.: intellectual contributor, study design

J. A. H.: intellectual contributor, study design, data analyses

B. Y.: intellectual contributor, study design, data analyses

A. L. R.: intellectual contributor, study design, data analyses

R. A. R.: intellectual contributor

S. D. G.: intellectual contributor

P. M. S.: principal investigator, co-author, intellectual contributor, study design, data analyses

Acknowledgments

This work was supported by National Institutes of Health Grants CA032685, CA87025, CA14520, GM067386, and T32-CA090217, grants from the Midwest Athletes for Childhood Cancer Fund, the Crawdaddy Foundation, The Evan Dunbar Foundation, the UW-Cure Kids Cancer Coalition, Abbie's Fund, St. Baldrick's Foundation, and the Super Jake Foundation. The authors thank Mrs. Kathleen Schell for flow cytometry support and helpful discussions.

Footnote

[1]INB and ZCN contributed equally to this study.

[2]INB is a lifetime member of the Association of Fellows of The International Union against Cancer (UICC), Geneva, Switzerland

[3] Gubbels JAA, Gadbaw B, Buhtoiarov IN, Horibata S, Kapur AK, Patel D, Hank JA, Gillies SD, Sondel PM, Connor J, Patankar MS. Ab-IL2 Fusion Proteins Mediate NK Cell Immune Synapse Formation by Polarizing CD25 to the Target Cell-Effector Cell Interface. Submitted to Journal of Leukocyte Biology as a companion manuscript to this report, 2010

References

1. Gillies, S.D., Reilly, E.B., Lo, K.M., Reisfeld, R.A. (1992) Antibody-targeted interleukin 2 stimulates T-cell killing of autologous tumor cells. *Proc Natl Acad Sci U S A* **89**, 1428-32.
2. Choi, B.S., Sondel, P.M., Hank, J.A., Schalch, H., Gan, J., King, D.M., Kendra, K., Mahvi, D., Lee, L.Y., Kim, K., Albertini, M.R. (2006) Phase I trial of combined treatment with ch14.18 and R24 monoclonal antibodies and interleukin-2 for patients with melanoma or sarcoma. *Cancer Immunol Immunother* **55**, 761-74.
3. Ritter, G., Livingston, P.O. (1991) Ganglioside antigens expressed by human cancer cells. *Semin Cancer Biol* **2**, 401-9.
4. Gilman, A.L., Ozkaynak, M.F., Matthay, K.K., Krailo, M., Yu, A.L., Gan, J., Sternberg, A., Hank, J.A., Seeger, R., Reaman, G.H., Sondel, P.M. (2009) Phase I study of ch14.18 with granulocyte-macrophage colony-stimulating factor and interleukin-2 in children with neuroblastoma after autologous bone marrow transplantation or stem-cell rescue: a report from the Children's Oncology Group. *J Clin Oncol* **27**, 85-91.
5. Lo Piccolo, M.S., Cheung, N.K., Cheung, I.Y. (2001) GD2 synthase: a new molecular marker for detecting neuroblastoma. *Cancer* **92**, 924-31.
6. Cheresh, D.A., Rosenberg, J., Mujoo, K., Hirschowitz, L., Reisfeld, R.A. (1986) Biosynthesis and expression of the disialoganglioside GD2, a relevant target antigen on small cell lung carcinoma for monoclonal antibody-mediated cytolysis. *Cancer Res* **46**, 5112-8.
7. Chang, H.R., Cordon-Cardo, C., Houghton, A.N., Cheung, N.K., Brennan, M.F. (1992) Expression of disialogangliosides GD2 and GD3 on human soft tissue sarcomas. *Cancer*

70, 633-8.

8. Lipinski, M., Braham, K., Philip, I., Wiels, J., Philip, T., Goridis, C., Lenoir, G.M., Tursz, T. (1987) Neuroectoderm-associated antigens on Ewing's sarcoma cell lines. *Cancer Res* **47**, 183-7.

9. Mennel, H.D., Bosslet, K., Geissel, H., Bauer, B.L. (2000) Immunohistochemically visualized localisation of gangliosides Glac2 (GD3) and Gtri2 (GD2) in cells of human intracranial tumors. *Exp Toxicol Pathol* **52**, 277-85.

10. King, D.M., Albertini, M.R., Schalch, H., Hank, J.A., Gan, J., Surfus, J., Mahvi, D., Schiller, J.H., Warner, T., Kim, K., Eickhoff, J., Kendra, K., Reisfeld, R., Gillies, S.D., Sondel, P. (2004) Phase I clinical trial of the immunocytokine EMD 273063 in melanoma patients. *J Clin Oncol* **22**, 4463-73.

11. Osenga, K.L., Hank, J.A., Albertini, M.R., Gan, J., Sternberg, A.G., Eickhoff, J., Seeger, R.C., Matthay, K.K., Reynolds, C.P., Twist, C., Krailo, M., Adamson, P.C., Reisfeld, R.A., Gillies, S.D., Sondel, P.M. (2006) A phase I clinical trial of the hu14.18-IL2 (EMD 273063) as a treatment for children with refractory or recurrent neuroblastoma and melanoma: a study of the Children's Oncology Group. *Clin Cancer Res* **12**, 1750-9.

12. Lode, H.N., Xiang, R., Dreier, T., Varki, N.M., Gillies, S.D., Reisfeld, R.A. (1998) Natural killer cell-mediated eradication of neuroblastoma metastases to bone marrow by targeted interleukin-2 therapy. *Blood* **91**, 1706-15.

13. Neal, Z.C., Yang, J.C., Rakhmilevich, A.L., Buhtoiarov, I.N., Lum, H.E., Imboden, M., Hank, J.A., Lode, H.N., Reisfeld, R.A., Gillies, S.D., Sondel, P.M. (2004) Enhanced activity of hu14.18-IL2 immunocytokine against murine NXS2 neuroblastoma when combined with interleukin 2 therapy. *Clin Cancer Res* **10**, 4839-47.

14. Lee, F.T., Rigopoulos, A., Hall, C., Clarke, K., Cody, S.H., Smyth, F.E., Liu, Z., Brechbiel, M.W., Hanai, N., Nice, E.C., Catimel, B., Burgess, A.W., Welt, S., Ritter, G., Old, L.J., Scott, A.M. (2001) Specific localization, gamma camera imaging, and intracellular trafficking of radiolabelled chimeric anti-G(D3) ganglioside monoclonal antibody KM871 in SK-MEL-28 melanoma xenografts. *Cancer Res* **61**, 4474-82.

15. Marlind, J., Kaspar, M., Trachsel, E., Sommavilla, R., Hindle, S., Bacci, C., Giovannoni, L., Neri, D. (2008) Antibody-mediated delivery of interleukin-2 to the stroma of breast cancer strongly enhances the potency of chemotherapy. *Clin Cancer Res* **14**, 6515-24.

16. Johnson, E.E., Lum, H.D., Rakhmilevich, A.L., Schmidt, B.E., Furlong, M., Buhtoiarov, I.N., Hank, J.A., Raubitschek, A., Colcher, D., Reisfeld, R.A., Gillies, S.D., Sondel, P.M. (2008) Intratumoral immunocytokine treatment results in enhanced antitumor effects. *Cancer Immunol Immunother* **57**, 1891-902.

17. Wagner, K., Schulz, P., Scholz, A., Wiedenmann, B., Menrad, A. (2008) The targeted immunocytokine L19-IL2 efficiently inhibits the growth of orthotopic pancreatic cancer. *Clin Cancer Res* **14**, 4951-60.

18. Duprez, V., Dautry-Varsat, A. (1986) Receptor-mediated endocytosis of interleukin 2 in a human tumor T cell line. Degradation of interleukin 2 and evidence for the absence of recycling of interleukin receptors. *J Biol Chem* **261**, 15450-4.

19. Fujii, M., Sugamura, K., Sano, K., Nakai, M., Sugita, K., Hinuma, Y. (1986) High-affinity receptor-mediated internalization and degradation of interleukin 2 in human T cells. *J Exp Med* **163**, 550-62.

20. Lowenthal, J.W., MacDonald, H.R., Iacopetta, B.J. (1986) Intracellular pathway of interleukin 2 following receptor-mediated endocytosis. *Eur J Immunol* **16**, 1461-3.

21. Hatakeyama, M., Mori, H., Doi, T., Taniguchi, T. (1989) A restricted cytoplasmic region of IL-2 receptor beta chain is essential for growth signal transduction but not for ligand binding and internalization. *Cell* **59**, 837-45.

22. Hatakeyama, M., Tsudo, M., Minamoto, S., Kono, T., Doi, T., Miyata, T., Miyasaka, M., Taniguchi, T. (1989) Interleukin-2 receptor beta chain gene: generation of three receptor forms by cloned human alpha and beta chain cDNA's. *Science* **244**, 551-6.

23. Baird, S.M. (2006) Part VIII Lymphocytes and plasma cells. Chapter 74. Morphology of lymphocytes and plasma cells. In *Williams Hematology* (M. A. Lichtman, W.J. Williams, E. Beutler, K. Kaushansky, T.J. Kipps, U. Seligsohn, J. Prchal, ed) McGraw-Hill Companies, Inc. 1023.

24. David, D., Bani, L., Moreau, J.L., Demaison, C., Sun, K., Salvucci, O., Nakarai, T., de Montalembert, M., Chouaib, S., Joussemet, M., Ritz, J., Theze, J. (1998) Further analysis of interleukin-2 receptor subunit expression on the different human peripheral blood mononuclear cell subsets. *Blood* **91**, 165-72.

25. Mailliard, R.B., Alber, S.M., Shen, H., Watkins, S.C., Kirkwood, J.M., Herberman, R.B., Kalinski, P. (2005) IL-18-induced CD83+CCR7+ NK helper cells. *J Exp Med* **202**, 941-53.

26. Kusano, A., Ohta, S., Shitara, K., Hanai, N. (1993) Immunocytochemical study on internalization of anti-carbohydrate monoclonal antibodies. *Anticancer Res* **13**, 2207-12.

27. Wargalla, U.C., Reisfeld, R.A. (1989) Rate of internalization of an immunotoxin correlates with cytotoxic activity against human tumor cells. *Proc Natl Acad Sci U S A* **86**, 5146-50.

28. Reisfeld, R.A. (1992) Potential of genetically engineered monoclonal antibodies for

cancer immunotherapy. *Pigment Cell Res* **Suppl 2**, 109-12.

29. Sondel, P.M., S.D. Gillies (2003) Immunocytokines for Cancer Immunotherapy. In *Handbook of cancer vaccines* (T. M. C. M.A. Morse, H.K. Lyerly, ed) Humana Press, Inc., Totowa, NJ p. 341-57.

30. Hank, J.A., Surfus, J.E., Gan, J., Jaeger, P., Gillies, S.D., Reisfeld, R.A., Sondel, P.M. (1996) Activation of human effector cells by a tumor reactive recombinant anti-ganglioside GD2 interleukin-2 fusion protein (ch14.18-IL2). *Clin Cancer Res* **2**, 1951-9.

31. Robertson, M.J., Cochran, K.J., Cameron, C., Le, J.M., Tantravahi, R., Ritz, J. (1996) Characterization of a cell line, NKL, derived from an aggressive human natural killer cell leukemia. *Exp Hematol* **24**, 406-15.

32. Imboden, M., Murphy, K.R., Rakhmilevich, A.L., Neal, Z.C., Xiang, R., Reisfeld, R.A., Gillies, S.D., Sondel, P.M. (2001) The level of MHC class I expression on murine adenocarcinoma can change the antitumor effector mechanism of immunocytokine therapy. *Cancer Res* **61**, 1500-7.

33. Hank, J.A., Robinson, R.R., Surfus, J., Mueller, B.M., Reisfeld, R.A., Cheung, N.K., Sondel, P.M. (1990) Augmentation of antibody dependent cell mediated cytotoxicity following in vivo therapy with recombinant interleukin 2. *Cancer Res* **50**, 5234-9.

34. Smith, K.A., Cantrell, D.A. (1985) Interleukin 2 regulates its own receptors. *Proc Natl Acad Sci U S A* **82**, 864-8.

35. Yu, A., Olosz, F., Choi, C.Y., Malek, T.R. (2000) Efficient internalization of IL-2 depends on the distal portion of the cytoplasmic tail of the IL-2R common gamma-chain and a lymphoid cell environment. *J Immunol* **165**, 2556-62.

36. Koch, A.M., Reynolds, F., Kircher, M.F., Merkle, H.P., Weissleder, R., Josephson, L.

(2003) Uptake and metabolism of a dual fluorochrome Tat-nanoparticle in HeLa cells. *Bioconjug Chem* **14**, 1115-21.

37. Ovejera, A.A., Houchens, D.P., Barker, A.D. (1978) Chemotherapy of human tumor xenografts in genetically athymic mice. *Ann Clin Lab Sci* **8**, 50-6.

38. Kim, Y., Kim, H.S., Cui, Z.Y., Lee, H.S., Ahn, J.S., Park, C.K., Park, K., Ahn, M.J. (2009) Clinicopathological implications of EpCAM expression in adenocarcinoma of the lung. *Anticancer Res* **29**, 1817-22.

39. Connor, J.P., Felder, M., Hank, J., Harter, J., Gan, J., Gillies, S.D., Sondel, P. (2004) Ex vivo evaluation of anti-EpCAM immunocytokine huKS-IL2 in ovarian cancer. *J Immunother* **27**, 211-9.

40. Went, P.T., Lugli, A., Meier, S., Bundi, M., Mirlacher, M., Sauter, G., Dirnhofer, S. (2004) Frequent EpCam protein expression in human carcinomas. *Hum Pathol* **35**, 122-8.

41. Hank, J.A., Surfus, J.E., Gan, J., Ostendorf, A., Gillies, S.D., Sondel, P.M. (2003) Determination of peak serum levels and immune response to the humanized anti-ganglioside antibody-interleukin-2 immunocytokine. *Methods Mol Med* **85**, 123-31.

42. Kendra, K., Gan, J., Ricci, M., Surfus, J., Shaker, A., Super, M., Frost, J.D., Rakhmilevich, A., Hank, J.A., Gillies, S.D., Sondel, P.M. (1999) Pharmacokinetics and stability of the ch14.18-interleukin-2 fusion protein in mice. *Cancer Immunol Immunother* **48**, 219-29.

43. Shusterman, S., London, W.B., Gillies, S.D., Hank, J.A., Voss, S., Seeger, R.C., Reynolds, C.P., Kimball, J., Albertini, M.A., Wagner, B., Gan, J., Eickhoff, J., DeSantes, K.D., Cohn, S.L., Hecht, T., Gadbaw, B., Reisfeld, R.A., Maris, J.M., Sondel, P.M. (2010) Anti-tumor activity of hu14.18-IL2 in relapsed/refractory neuroblastoma patients: a

Children's Oncology Group (COG) phase II study. J Clin Oncology. In press, PMID: 20921469

Figure 1

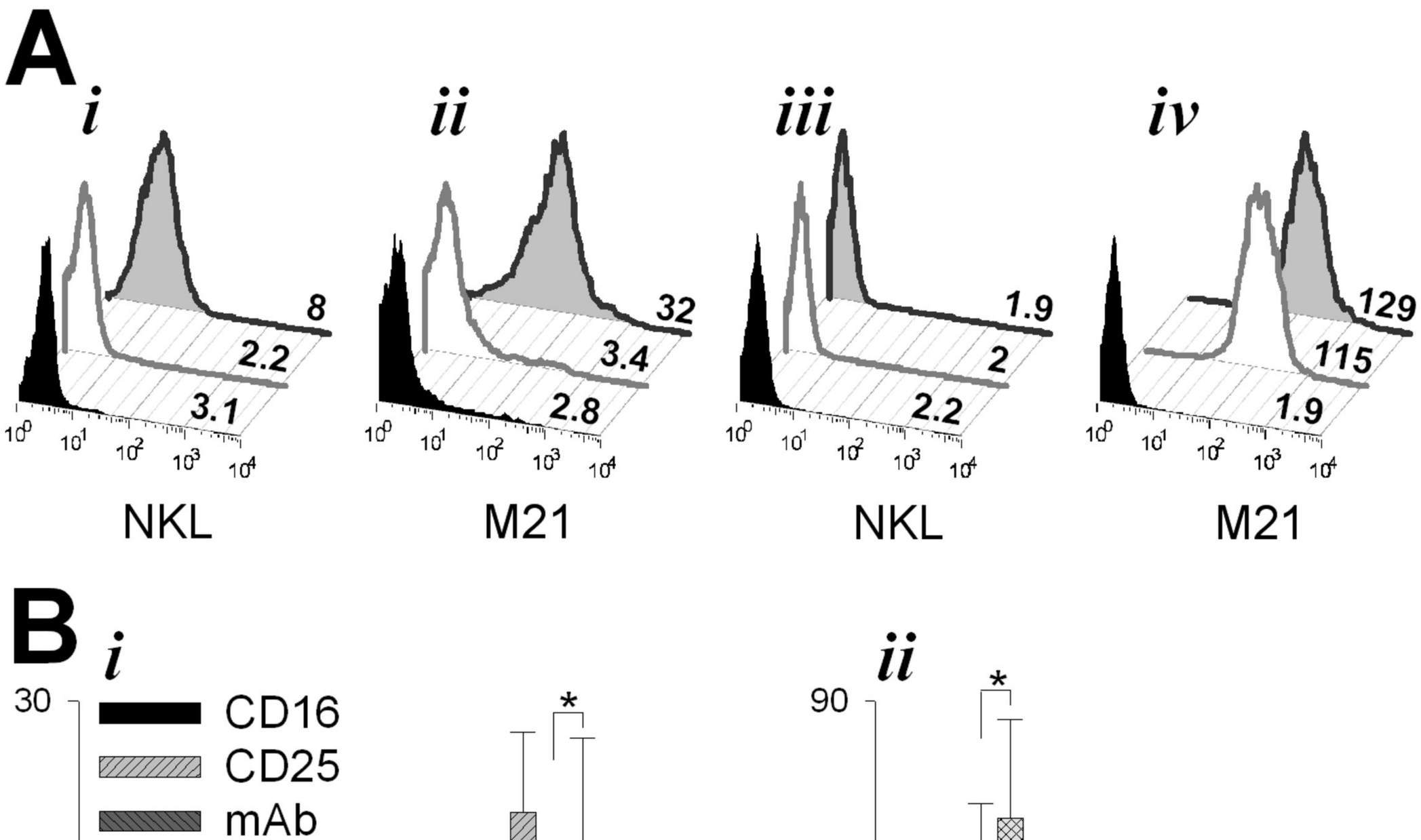
A
i
ii
iii
iv
8
2.2
3.1
32
3.4
2.8
1.9
2
2.2
129
115
1.9
10^0 10^1 10^2 10^3 10^4
NKL
M21
NKL
M21
B
i
CD16
CD25
mAb
IC
MFI ratio
30
20
10
0
*
#
NKL
RL12
L5178Y
K562
ii
90
60
30
0
M21
NXS2
CT26

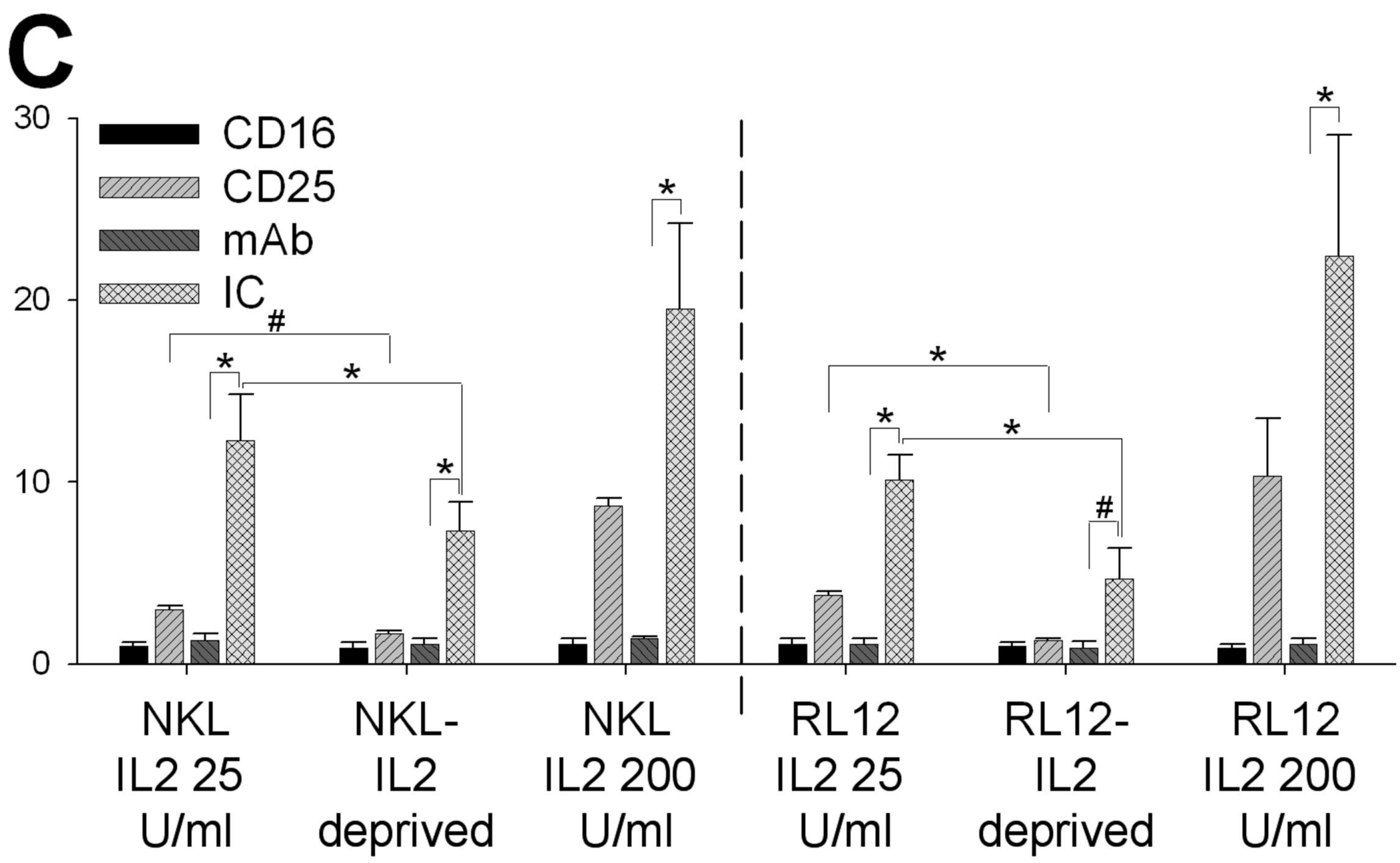
C
CD16
CD25
mAb
IC
MFI ratio
30
20
10
0
*
#
NKL
IL2 25 U/ml
NKL-IL2 deprived
NKL
IL2 200 U/ml
RL12
IL2 25 U/ml
RL12-IL2 deprived
RL12
IL2 200 U/ml

Figure 2

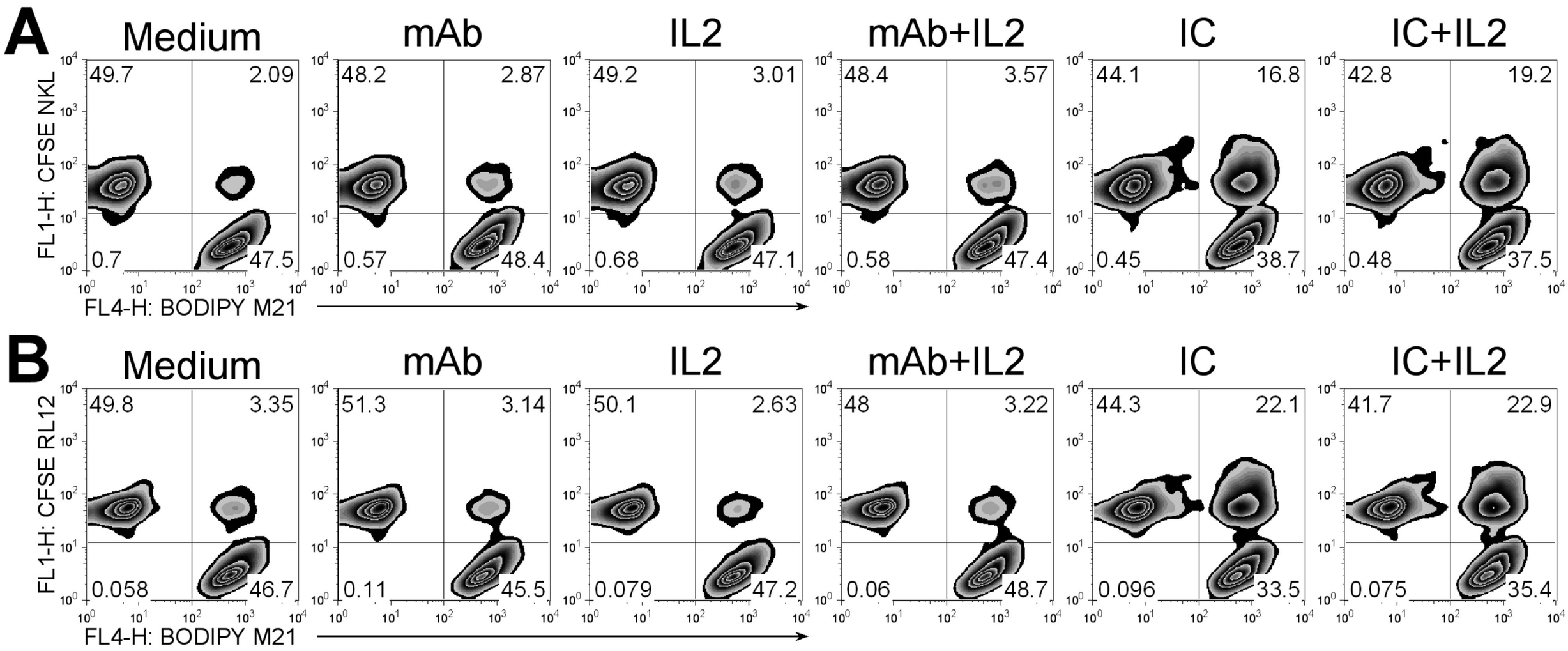
A
Medium
mAb
IL2
mAb+IL2
IC
IC+IL2
FL1-H: CFSE NKL
FL4-H: BODIPY M21
49.7
2.09
0.7
47.5
48.2
2.87
0.57
48.4
49.2
3.01
0.68
47.1
48.4
3.57
0.58
47.4
44.1
16.8
0.45
38.7
42.8
19.2
0.48
37.5
B
Medium
mAb
IL2
mAb+IL2
IC
IC+IL2
FL1-H: CFSE RL12
FL4-H: BODIPY M21
49.8
3.35
0.058
46.7
51.3
3.14
0.11
45.5
50.1
2.63
0.079
47.2
48
3.22
0.06
48.7
44.3
22.1
0.096
33.5
41.7
22.9
0.075
35.4

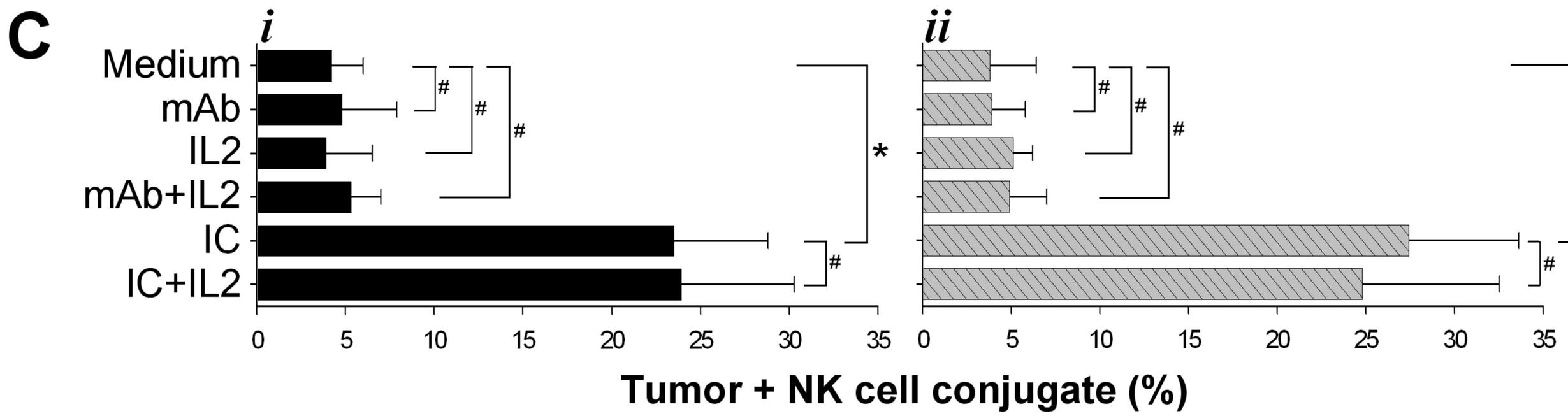
C
i
ii
Medium
mAb
IL2
mAb+IL2
IC
IC+IL2
#
*
0
5
10
15
20
25
30
35
Tumor + NK cell conjugate (%)

Figure 3

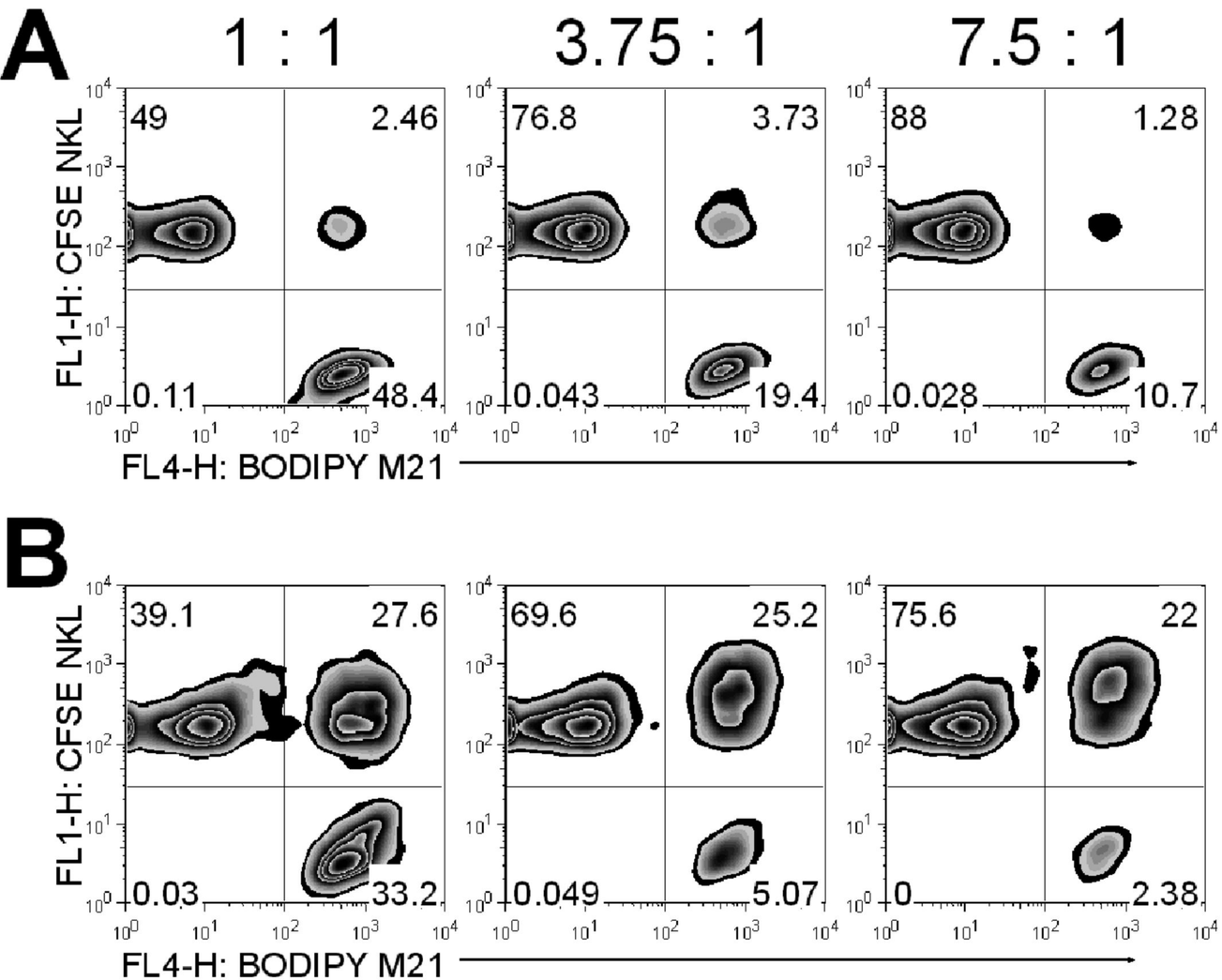
A
1 : 1
3.75 : 1
7.5 : 1
49
2.46
0.11
48.4
76.8
3.73
0.043
19.4
88
1.28
0.028
10.7
FL1-H: CFSE NKL
FL4-H: BODIPY M21
B
39.1
27.6
0.03
33.2
69.6
25.2
0.049
5.07
75.6
22
0
2.38
FL1-H: CFSE NKL
FL4-H: BODIPY M21

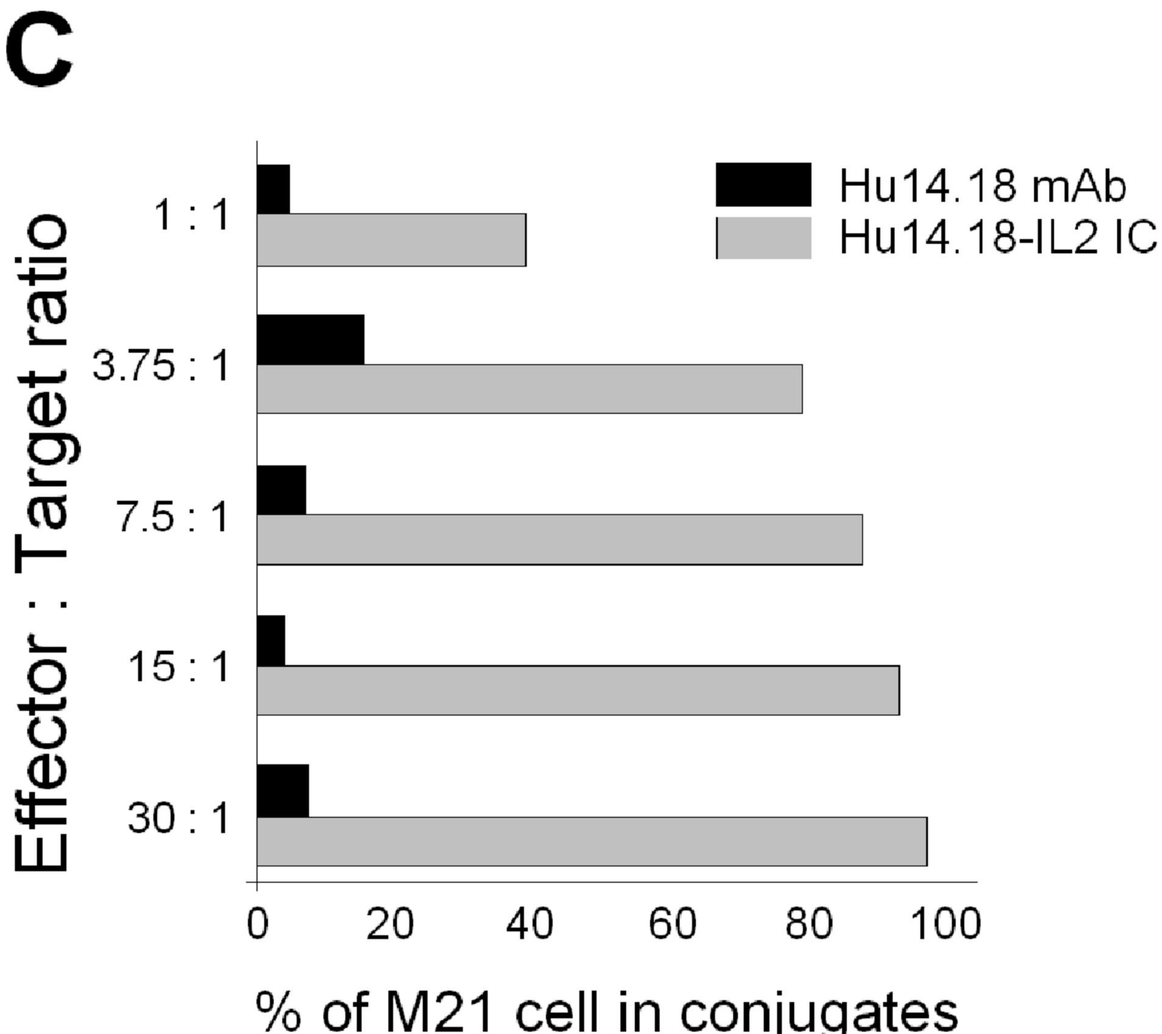
C
Hu14.18 mAb
Hu14.18-IL2 IC
Effector : Target ratio
1 : 1
3.75 : 1
7.5 : 1
15 : 1
30 : 1
0
20
40
60
80
100
% of M21 cell in conjugates

Figure 4

A

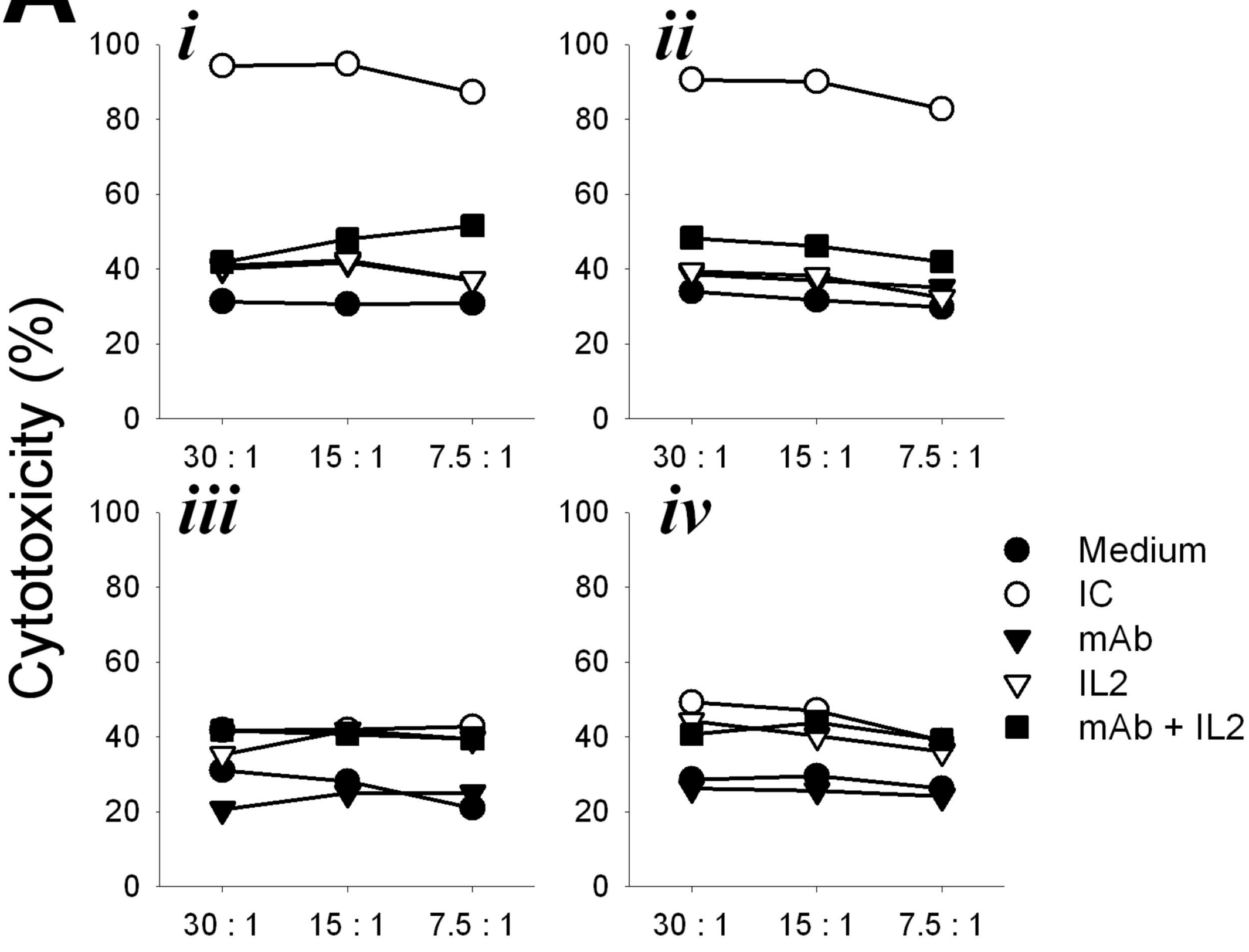
i
ii
iii
iv
100
80
60
40
20
0
30 : 1
15 : 1
7.5 : 1
Cytotoxicity (%)
E/T ratio
Medium
IC
mAb
IL2
mAb + IL2

B

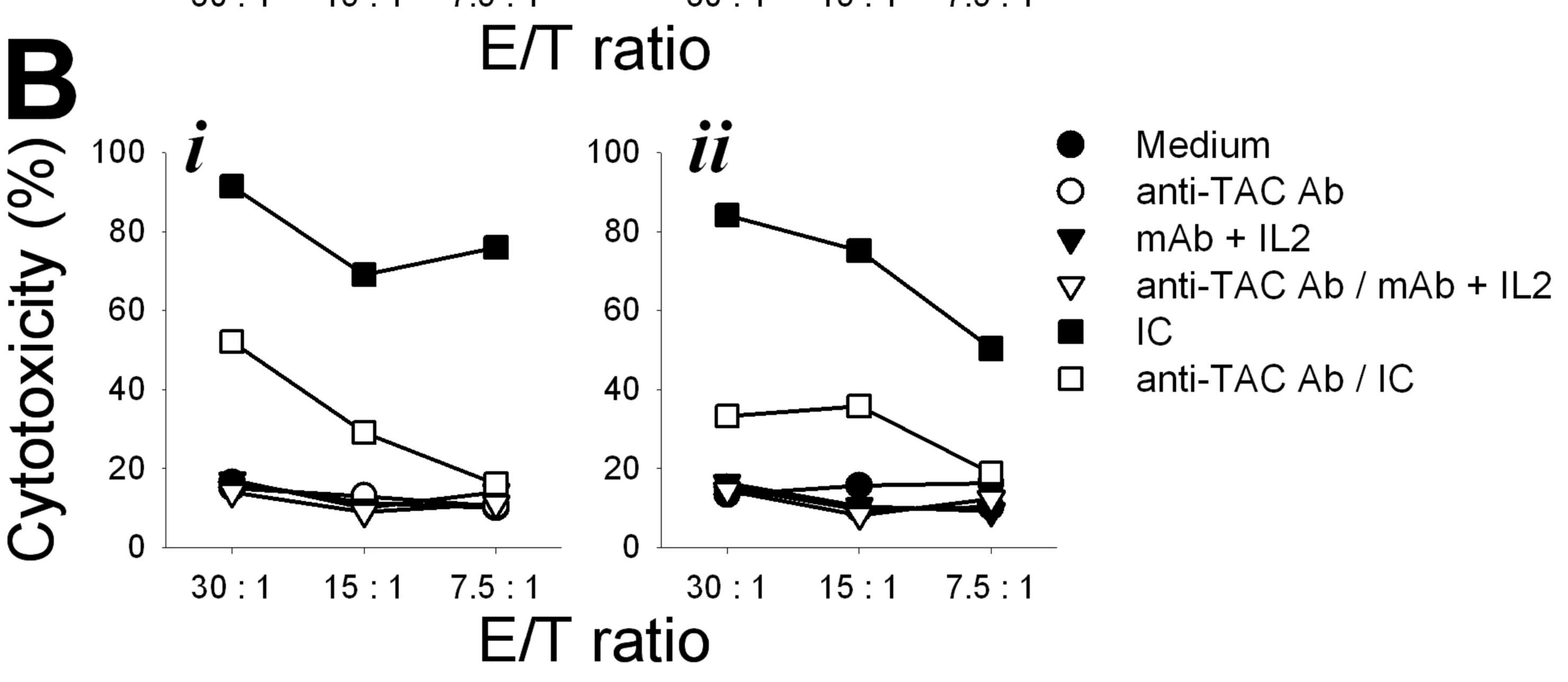
i
ii
100
80
60
40
20
0
30 : 1
15 : 1
7.5 : 1
Cytotoxicity (%)
E/T ratio
Medium
anti-TAC Ab
mAb + IL2
anti-TAC Ab / mAb + IL2
IC
anti-TAC Ab / IC

Figure 5

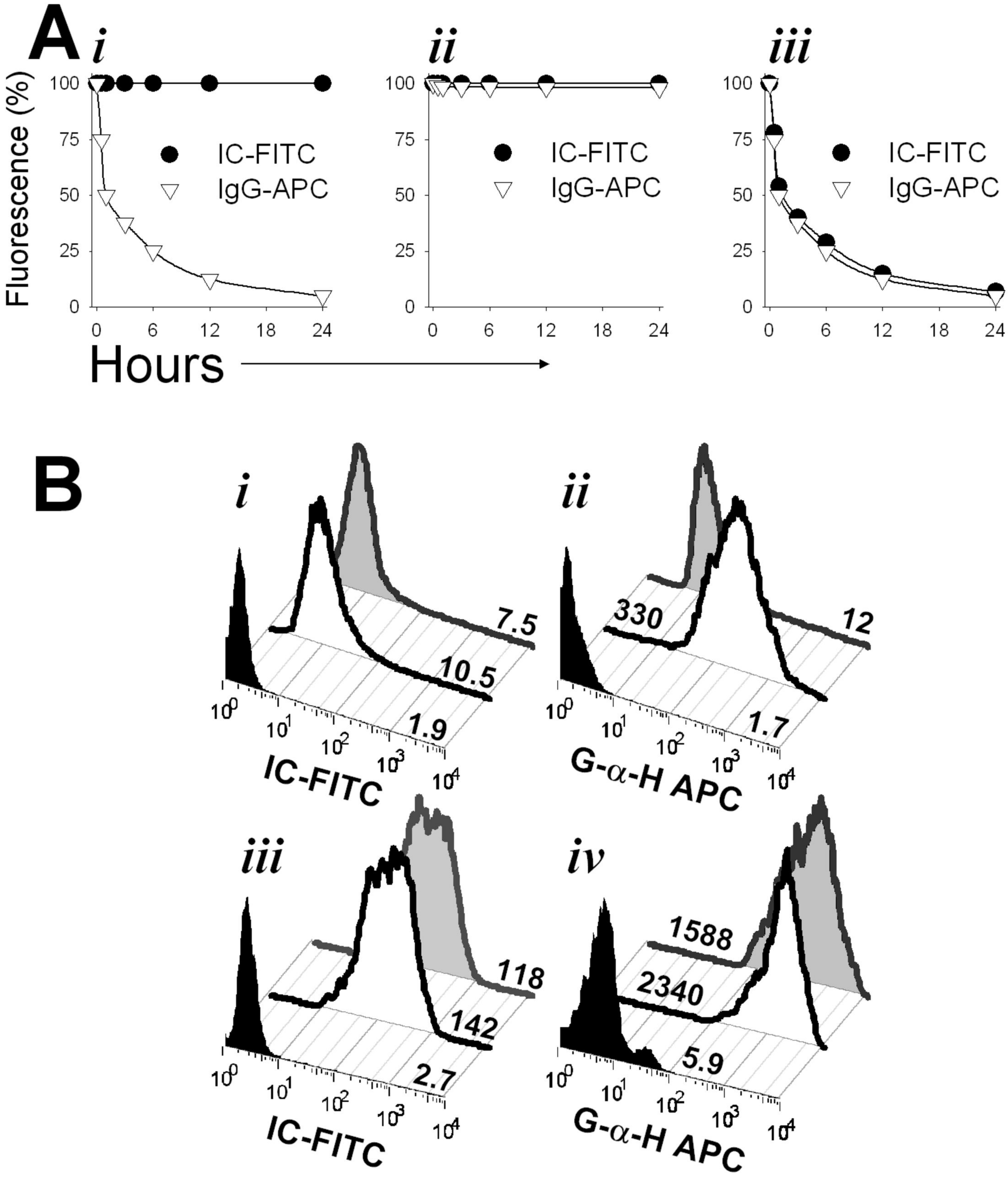
A
i
ii
iii
Fluorescence (%)
100
75
50
25
0
0
6
12
18
24
IC-FITC
IgG-APC
Hours
B
i
ii
iii
iv
7.5
10.5
1.9
330
12
1.7
118
142
2.7
1588
2340
5.9
10^0
10^1
10^2
10^3
10^4
IC-FITC
G-α-H APC
C
i
ii
iii
iv
v
vi
M21
NXS2
L5178Y
IL2 200 U/ml
IL2 25 U/ml
IL2-deprived
Fluorescence (%)
Hours

Figure 6

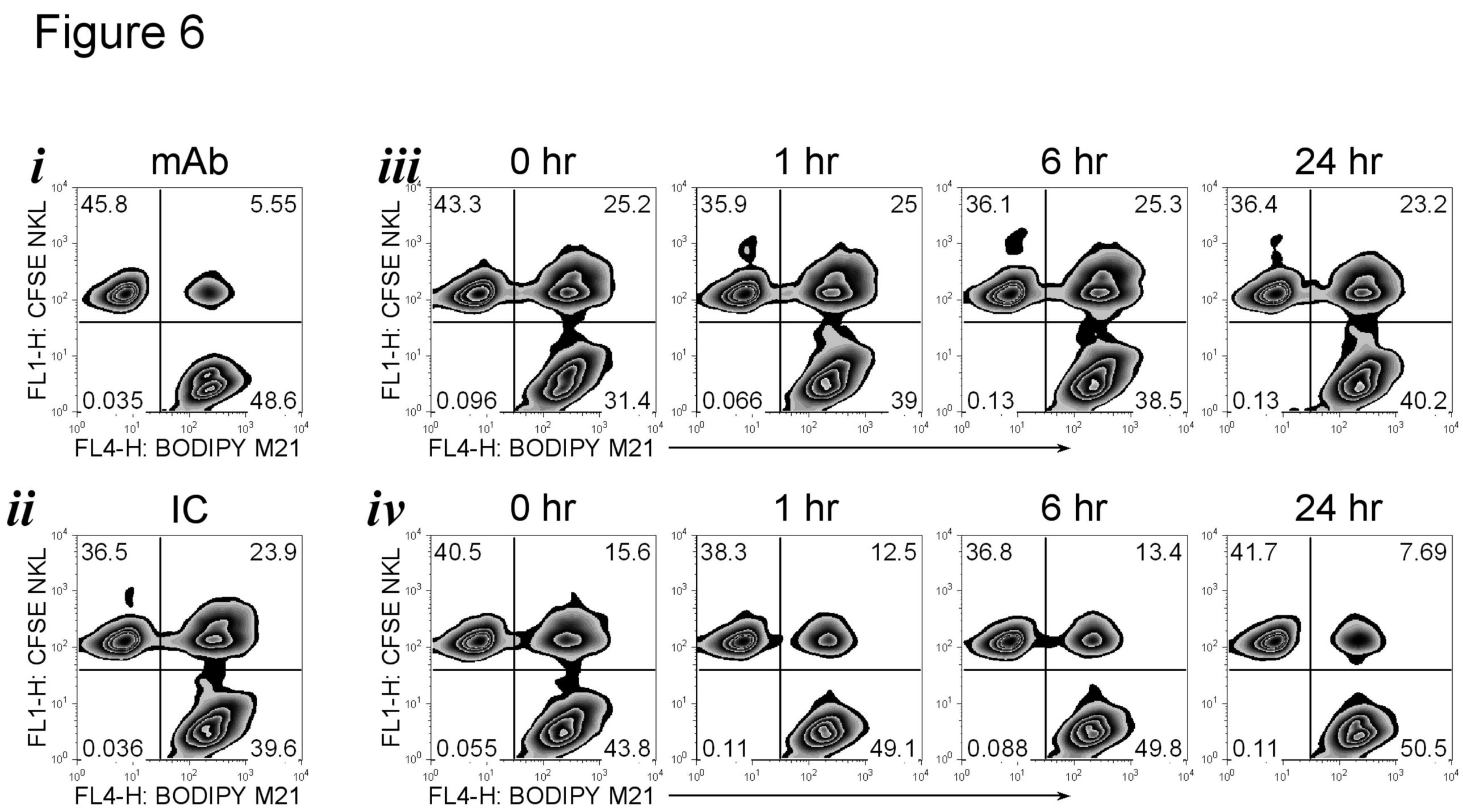
i
mAb
45.8
5.55
0.035
48.6
FL1-H: CFSE NKL
FL4-H: BODIPY M21
iii
0 hr
1 hr
6 hr
24 hr
43.3
25.2
0.096
31.4
35.9
25
0.066
39
36.1
25.3
0.13
38.5
36.4
23.2
0.13
40.2
FL1-H: CFSE NKL
FL4-H: BODIPY M21
ii
IC
36.5
23.9
0.036
39.6
FL1-H: CFSE NKL
FL4-H: BODIPY M21
iv
0 hr
1 hr
6 hr
24 hr
40.5
15.6
0.055
43.8
38.3
12.5
0.11
49.1
36.8
13.4
0.088
49.8
41.7
7.69
0.11
50.5
FL1-H: CFSE NKL
FL4-H: BODIPY M21

Figure 7

A

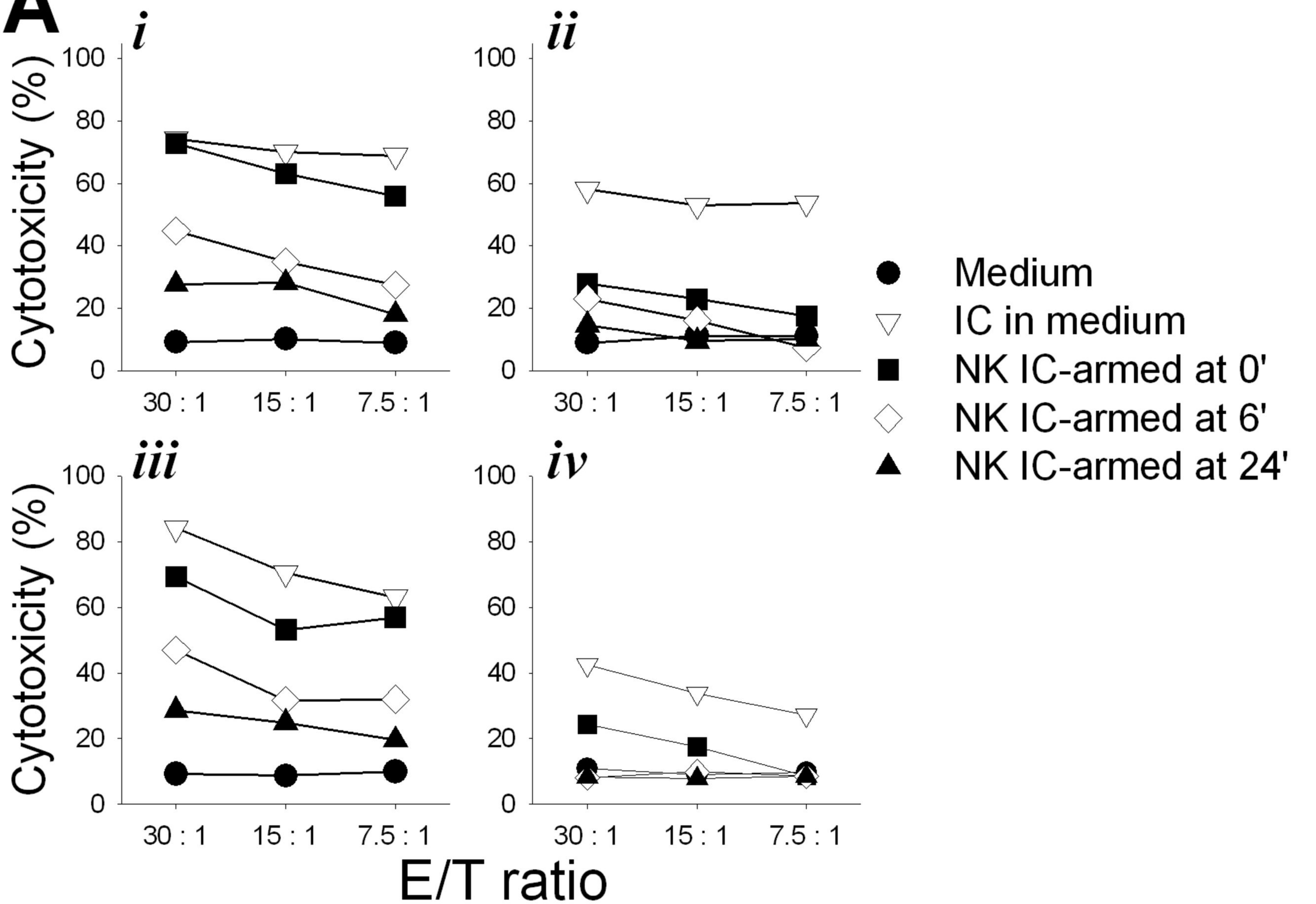
i
ii
iii
iv
Cytotoxicity (%)
100
80
60
40
20
0
30 : 1
15 : 1
7.5 : 1
E/T ratio
Medium
IC in medium
NK IC-armed at 0'
NK IC-armed at 6'
NK IC-armed at 24'

B

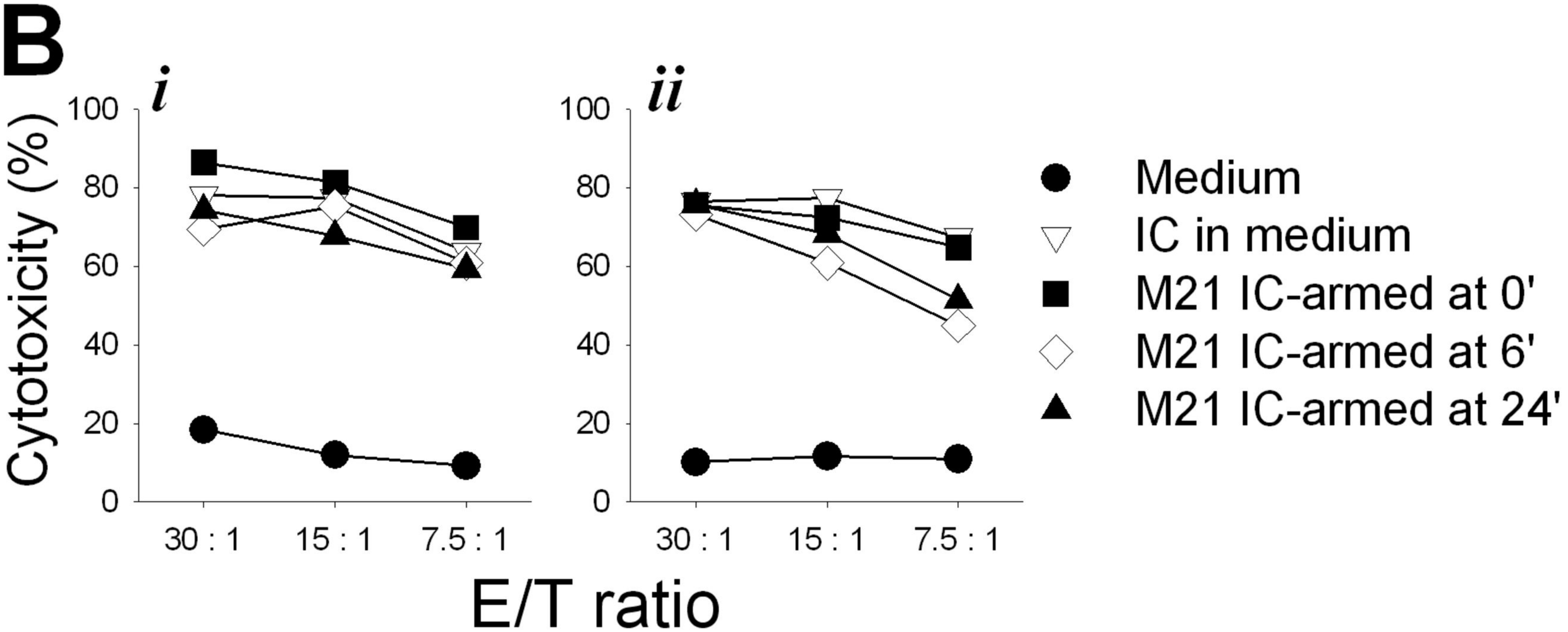
i
ii
Cytotoxicity (%)
100
80
60
40
20
0
30 : 1
15 : 1
7.5 : 1
E/T ratio
Medium
IC in medium
M21 IC-armed at 0'
M21 IC-armed at 6'
M21 IC-armed at 24'

Figure 8

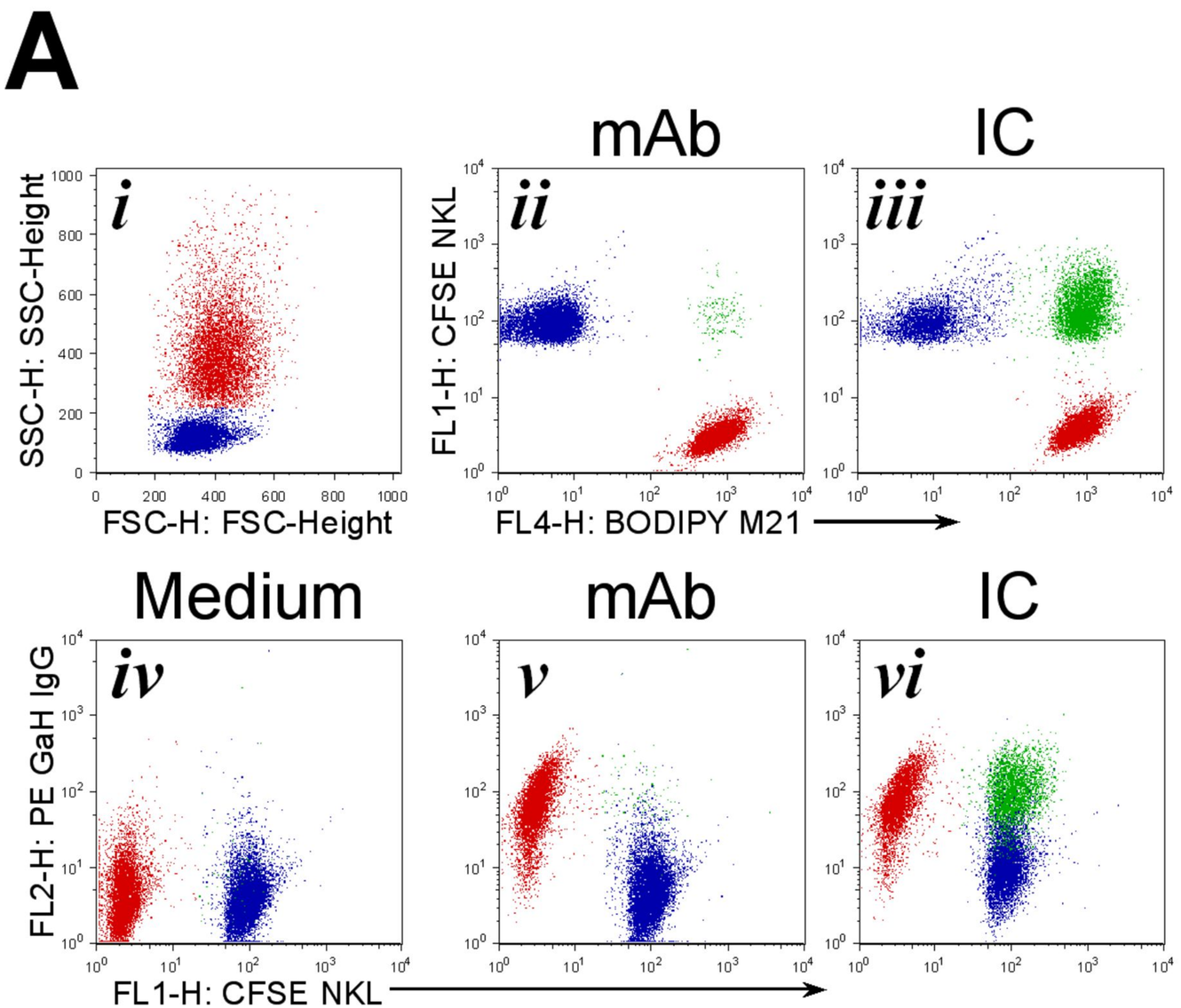
A
mAb
IC
i
ii
iii
SSC-H: SSC-Height
FSC-H: FSC-Height
FL1-H: CFSE NKL
FL4-H: BODIPY M21
Medium
mAb
IC
iv
v
vi
FL2-H: PE GaH IgG
FL1-H: CFSE NKL

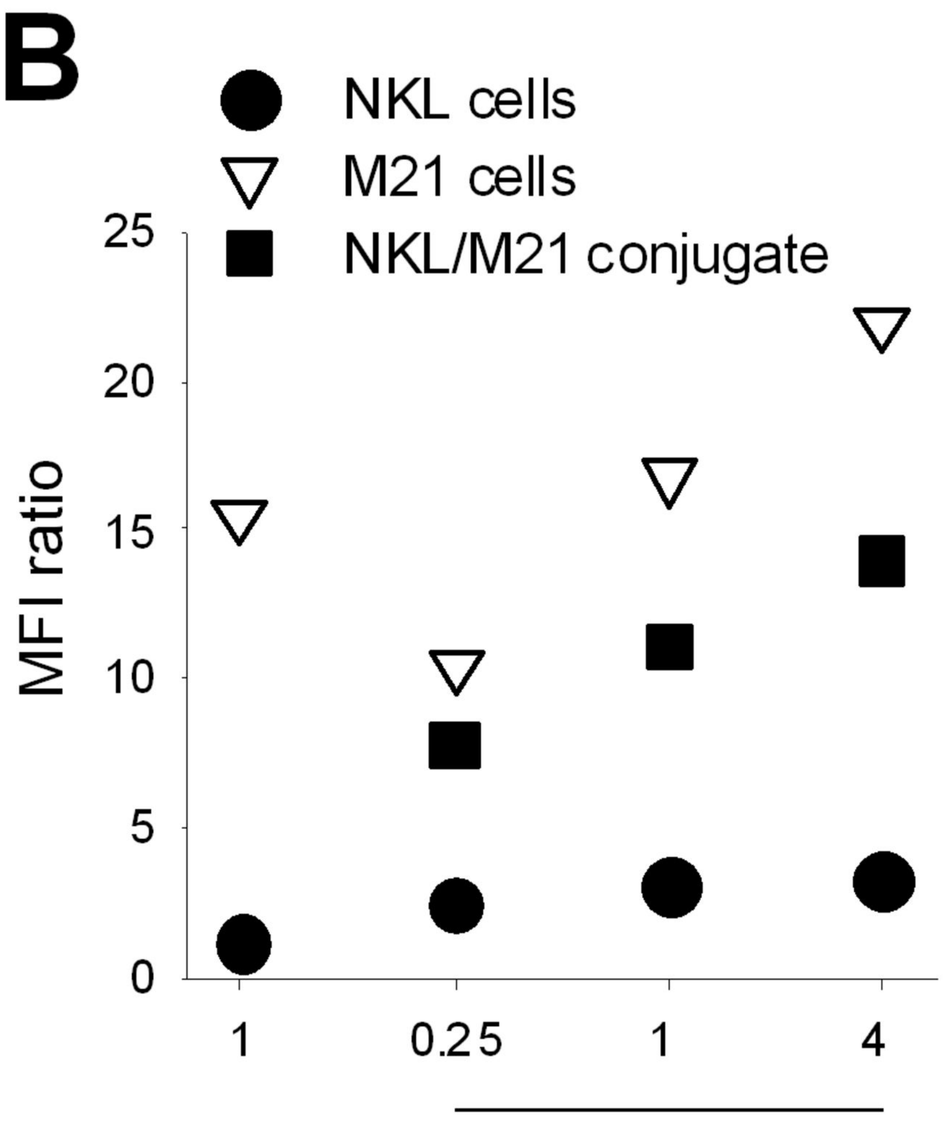
B
NKL cells
M21 cells
NKL/M21 conjugate
MFI ratio
25
20
15
10
5
0
1
0.25
1
4
14.18 mAb
IC

Figure 9

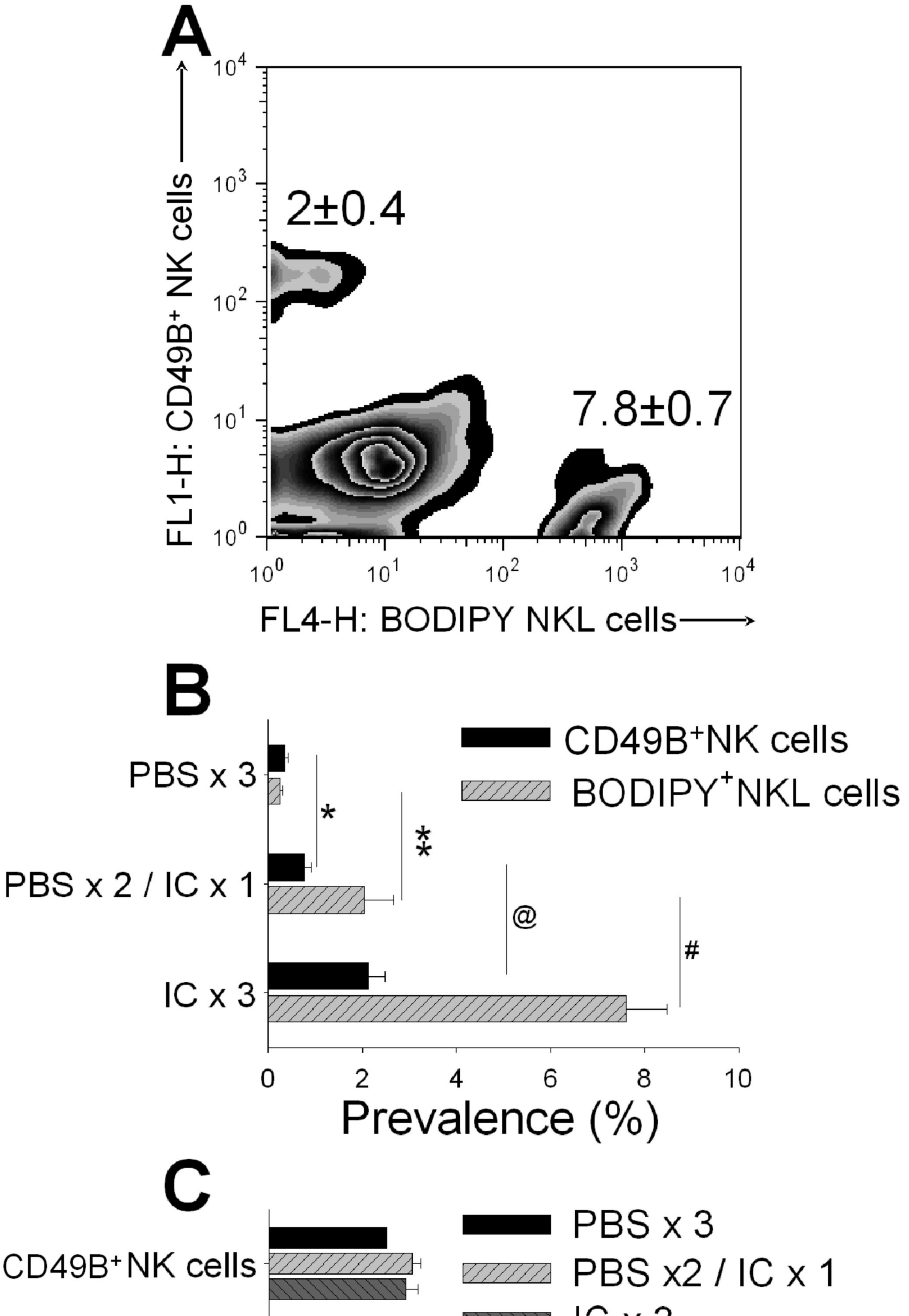
A
FL1-H: CD49B+ NK cells
10^4
10^3
10^2
10^1
10^0
2±0.4
7.8±0.7
10^0
10^1
10^2
10^3
10^4
FL4-H: BODIPY NKL cells
B
CD49B+NK cells
BODIPY+NKL cells
PBS x 3
PBS x 2 / IC x 1
IC x 3
*
**
@
#
0
2
4
6
8
10
Prevalence (%)
C
CD49B+ NK cells
BODIPY+ NKL cells
CD49B-/BODIPY-
tumor cells/stroma
PBS x 3
PBS x2 / IC x 1
IC x 3
0
1
2
3
4
MFI ratio